Developmental tracing of *lhb* gene expression in medaka (*Oryzias latipes*) using the stable tg(*lhb*:GFP) line and generation of a corresponding tg(*fshb*:RFP) line

Master thesis by Rikke Lifjeld

The Physiology Programme

Department of Molecular Biosciences

Faculty of Mathematics and Natural Sciences

UNIVERSITY OF OSLO

2011

Acknowledgements

Først og fremst vil jeg takke mine veiledere Finn-Arne Weltzien, Jon Hildahl og Trude M. Haug. Takk for at dere har introdusert meg for forskningens verden. På grunn av deres gode veiledning og mange råd har jeg fått oppleve hvor fantastisk det er å få gode resultater, samtidig som dere har hjulpet meg gjennom perioder hvor ting ikke har gått like greit. Jeg vil spesielt takke Jon for et godt samarbeid, mange gode diskusjoner og for at han har vært tålmodig og lært meg opp i nye metoder på lab.

Jeg vil også takke for at jeg har fått vært en del av vår fantastiske forskningsgruppe! Her er alle behjelpelige med gode faglige diskusjoner og alle bidrar til en sosial og hyggelig hverdag på lab. Tusen takk til Kristine for «studietur» til Nederland, og for gjennomlesning av oppgaven. Takk til Gunnveig, Stine og Line for gode kollokvier og godt samhold som de «nye» masterstudentene. Takk Kjetil, for at du lærte meg å mikroinjisere og for faglige diskusjoner.

Takk til alle studievenner gjennom 5 år på Blindern. Maria og Saranda, disse årene ville ikke vært det samme uten dere. Takk for flotte minner fra studietiden.

Tusen takk for god støtte fra familie og venner, og for at dere har holdt ut alt snakket om fiskeeggene mine. En spesiell takk til mamma som er en god lytter og alltid stiller opp.

Rikke Lifjeld

Oslo, desember 2011

Abstract

Luteinizing hormone (LH) and follicle-stimulating hormone (FSH) are gonadotropic hormones produced in the anterior pituitary by gonadotrope cells. These hormones are key regulators of vertebrate reproduction because of their effects on gonadal steroidogenesis and gametogenesis. Even though these hormones are key components of the brain-pituitary-gonad axis, which controls reproduction in all vertebrates, the regulation of these two hormones and the embryonic development of gonadotrope cells, are poorly understood. To better characterize the embryonic development of gonadotrope cells and their regulation at puberty, we wanted to develop stable transgenic lines of medaka with the gonadotropic hormone promotors (for *lhb* and *fshb*) driving fluorescent proteins. The tg(*lhb*:GFP) line already established by the group with the *lhb* promotor driving green fluorescent protein (Gfp) expression, was used to trace the development of LH gonadotropes using fluorescent light and confocal microscopy in whole larvae. Additionally, qPCR was used to measure developmental *lhb* gene expression. An additional project in this thesis was to develop a transgenic medaka line with the *fshb* promotor driving red fluorescent protein (Rfp). The *fshb* promotor sequence was ligated into a pBluescript II SK vector upstream of the *rfp* (mCherry) insert. The tg(*fshb*:RFP) construct was later microinjected into one cell stage embryos, which were screened for fluorescent expression and grown to sexual maturity.

Table of content

Abbreviations

The nomenclature for gene and protein names used in this thesis is concurrent with the nomenclature described for zebrafish (www.zfin.org), i.e. gene names in lowercase italics and protein names in non-italics with the first letter in uppercase. Transgenic lines and constructs will be termed tg(promotor:gene). Genes and proteins discussed in mammals have normal nomenclature.

ACTH	adrenocorticotropic hormone
ANOVA	analysis of variance
BAC	bacterial artificial chromosome
bp	base pairs
BPG	brain-pituitary-gonad
cDNA	complementary deoxy robinucleic acid
CG	placenta specific chorionic gonadotropin
CNS	central nervous system
Cq	quantification cycle
DIG	digoxigenin
DNA	deoxy ribonucleic acid
dNTP	deoxy ribonucleotide triphosphate
dpf	days post fertilization
DTT	dithiothreitol
E3 medium	5 mM NaCl, 0.17 mM KCl, 0.33 mM$CaCl_2$, 0.33 mM $MgSO_4$ and methylene blue

FSH	follicle-stimulating hormone
FSH-R	FSH receptor
GABA	gamma-amino butyric acid
gDNA	genomic DNA
GFP	green flourescent protein
GnRH	gonadotropin-releasing hormone
GPA	glycoprotein alpha
GPA2	glycoprotein alpha 2
GPB5	glycoprotein beta 5
hpf	hours post fertilization
IPTG	isopropyl-beta-D-thiogalactopyranoside
ISH	in situ hybridization
kb	kilobases
KDS	potassium dodecyl sulfate
LB	lysogeny broth (bacterial growth medium)
LH	luteinizing hormone
LH-R	LH receptor
MCS	multiple cloning site
MSH	melanocyte-stimulating hormone
mRNA	messenger RNA
NTC	non template control

PBS	phosphate buffered saline
PCR	polymerase chain reaction
PD	pars distalis
PFA	paraformaldehyde
PI	pars intermedia
PN	pars nervosa
PPD	posterior pars distalis
ppe	preplacodal ectoderm
qPCR	quantitative PCR
RFP	red flourescent protein
RIN	RNA integrity number
RNA	ribonucleic acid
RPD	rostral pars distalis
rRNA	ribosomal RNA
rt	reverse transcriptase
SOC	super optimal broth with catabolite repression
tg	transgene
TSH	thyroid stimulating hormone
X-Gal	5-bromo-4-chloro-3-indolyl-beta-D-galacto-pyranoside

1 Introduction

The host for my master thesis, the Weltzien-Haug research group, studies the physiological control mechanisms involved in reproduction, focusing on the gonadotropin-producing cells (gonadotropes) in the pituitary and how they function. The gonadotrope cells synthesize and secrete two gonadotropins, follicle-stimulating hormone (FSH) and luteinizing hormone (LH). FSH and LH constitute an important part of the brain-pituitary-gonad (BPG) axis, the endocrine axis that regulates vertebrate puberty and reproduction (see below). Little is known, however, regarding the possible function of gonadotropins during early development. Using a recently generated Gfp-transgenic medaka line, it has for the first time in a vertebrate been possible to follow the spatial and temporal expression of a gonadotropin (Lh, fish protein, *lhb* fish gene) during embryonic development. This project also included work on generating a second transgenic line for the detection of Fsh protein *(fshb* gene) to gain further insight into the expression and function of gonadotropic hormones during early development.

1.1 Brain-Pituitary-Gonad (BPG) axis

The BPG axis consists of three physiologically connected components, the hypothalamus in the brain, the pituitary and the gonads (figure 1). The BPG axis is vital to reproductive maturation in all vertebrates and the basic organization of the axis is highly conserved (Al-Kindi et al., 2001; Lake et al., 2008). Information from external and internal sources is integrated in the brain, which conveys an output in the form of gonadotropin-releasing hormone (GnRH) to the pituitary where synthesis and secretion of the gonadotropic hormones, LH and FSH, are modulated accordingly. The pulsatile secretion of GnRH was believed to be found in all vertebrate species (Dellovade et al., 1998). This is true for mammals (for review, see Millar et al., 2004), but there is no conclusive evidence for this pulsatility in fish. FSH and LH bind to their cognate receptors and regulate the two main activities of the gonads, steroidogenesis and gametogenesis (Schulz and Goos, 1999). Gonadal sex steroids control the different stages of gametogenesis together with FSH, while LH mainly controls steroidogenesis. These sex steroids can have a positive or negative feedback on the pituitary and the brain depending on the maturational state of the organism (Schulz and Goos, 1999). In fish, the most important androgen and estrogen are 11-ketotestosterone and 17β-estradiol, respectively (for review, see Borg, 1994).

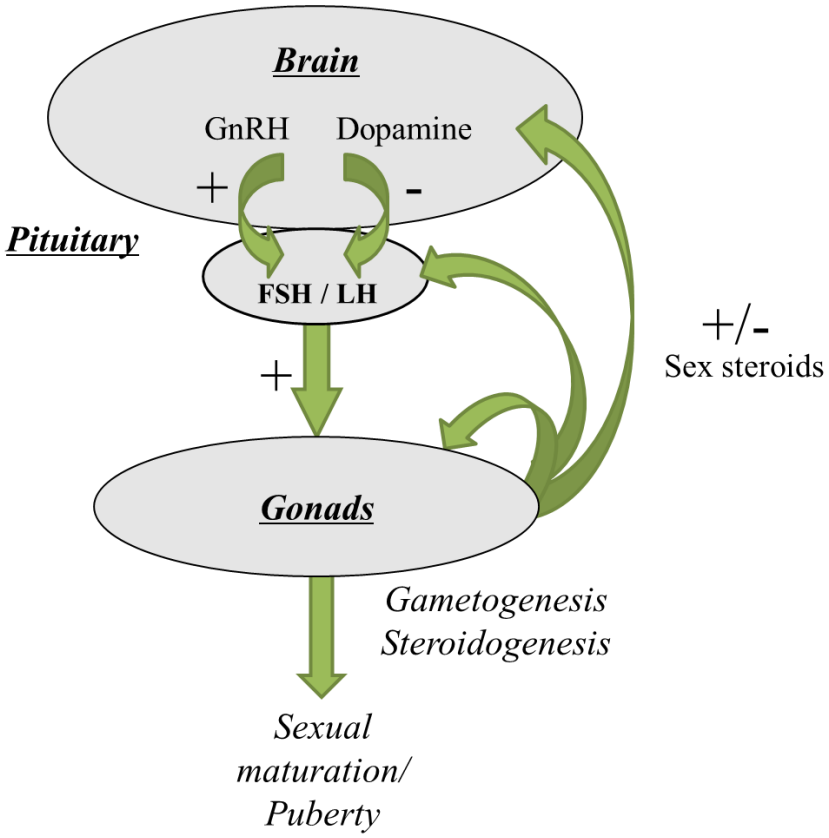

Figure 1 Brain-Pituitary-Gonad (BPG) axis. This figure shows a simplified version of the BPG axis in teleosts. Stimulating and inhibiting signals produce an integrated output in the brain, resulting in the release of the stimulatory GnRH and the inhibitory dopamine. GnRH binds to receptors in the pituitary, and activation of these receptors leads to synthesis and release of FSH and LH. Dopamine can either bind to receptors on the gonadotropes or on the cells producing GnRH, directly or indirectly leading to inhibition of FSH and/or LH release. FSH and LH act on target cells in the gonads, and initiate the production of sperm and eggs (gametogenesis), in addition to synthesis and secretion of steroid hormones (steroidogenesis). The sex steroids can have a positive or negative feedback on the pituitary and the brain, depending on the maturational stage.

Dopamine is a catecholamine neurotransmitter that is shown in some species to oppose the effect of GnRH by inhibiting production and release of gonadotropins indirectly via GnRH neurons, but also directly at the pituitary level as indicated by the expression of dopamine receptors in gonadotropes. This is the case in several teleost species (Chang and Peter, 1983; Chang et al., 1990; De Leeuw et al., 1988; Vidal et al., 2004; Yu et al., 1991). The BPG axis is not only influenced by the feedback mechanisms within the axis itself. To ensure that reproduction takes place when the conditions for offspring survival are optimal, the BPG axis is influenced by various external and internal factors. Examples of external factors that have been shown to influence the BPG axis include temperature, availability of food, population density, photoperiod, lunar phase and pheromones, whereas internal factors include those

related to nutritional status, such as leptin, ghrelin, and neurohormones like neuropeptide Y, GABA, norepinephrine and various RF-amides (Bromage et al., 2001; Burnard et al., 2008; Evans and Claiborne, 2006; Kobayashi et al., 2002; Levavi-Sivan et al., 2010; Schulz and Goos, 1999; Tena-Sempere and Barreiro, 2002). During the transformation from a sexually immature juvenile to a mature adult, the BPG axis achieves its full hormonal and gametogenetic capacity (Norris, 1997). In teleosts, like in other vertebrates, it seems that an activation of the GnRH system is a key event in the onset of puberty. However, how and when this activation occurs is not fully explained in any vertebrate (Schulz and Goos, 1999; Taranger et al., 2010).

1.2 The Pituitary

Both in teleosts and other vertebrates, including mammals, the pituitary consists of two parts, a posterior part (posterior pituitary, neurohypophysis), which derives from the ventral diencephalon, and an anterior part (anterior pituitary, adenohypophysis), which have an ectoderm origin.

1.2.1 Anatomy

The vertebrate pituitary is situated in a bony chamber, *sella turcica*, situated posterior to the optic chiasm and below the hypothalamus (Frisen, 1967). The teleost anterior pituitary can be divided into two different compartments; the anteriorly located *pars distalis* (PD) and the posteriorly located *pars intermedia* (PI). PD can further be divided into *rostral* (anterior) *pars distalis* (RPD) and *proximal pars distalis* (PPD) (figure 2) (Frisen, 1967; Levavi-Sivan et al., 2010; Schreibman et al., 1973; Weltzien et al., 2004). The portal system that transports neurohormonal regulators from the hypothalamus to the pituitary in mammals is absent in teleost fish. Instead, fish have direct axonal transport of the neurohormonal regulators from the hypothalamic neurons to the endocrine cells in the pituitary, through the neurohypophysis (*pars nervosa*, PN) (Ball and Baker, 1969).

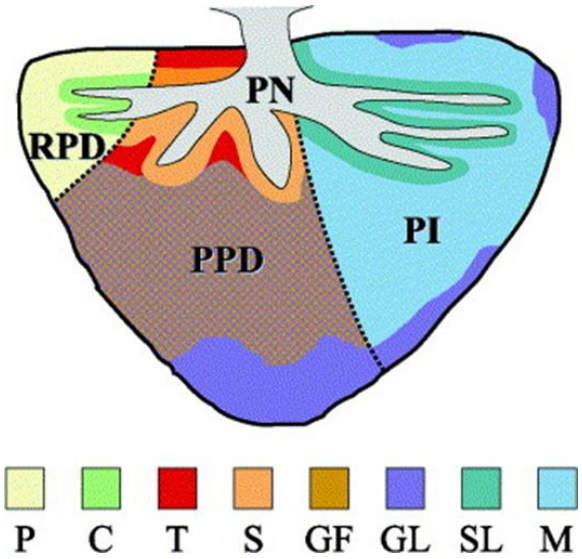

Figure 2 A schematic diagram of the Atlantic Halibut pituitary. Ball and Baker (1969), states that the anatomy of the pituitary gland in teleosts have a common anatomical pattern as seen here in the Atlantic halibut. The different hormone-producing cell types have a specific localization in the pituitary. Both FSH- and LH-producing gonadotropes can be found in the periphery of the PPD and the PI. Abbreviations: P = lactotropes, C = corticotropes, T = thyrotropes, S = somatotropes, GF = FSH-producing gonadotropes, GL = LH-producing gonadotropes, SL = somatolactotropes, M = melanotropes, RPD = *rostral pars distalis*, PPD = *proximal pars distalis*, PI = *pars intermedia* and PN = *pars nervosa*. From Weltzien et al. (2004).

The organization of specialized cell types in the pituitary differs between tetrapods and teleosts. In teleosts, there is a compartmental organization of the cells with each specific hormone-producing cell type located in a specific pituitary compartment (Ball and Baker, 1969; Schreibman et al., 1973). The same compartmental organization occurs in tetrapods in the embryonic stages, while in adults, the cells are distributed in a mosaic pattern (for reviews, see Doerr-Schott, 1976; Voss and Rosenfeld, 1992; Weltzien et al., 2004).

1.2.2 Cell types in the pituitary

There are six different cell types in the anterior pituitary of most vertebrates, while in the anterior pituitary of teleosts there are eight different cell types. This is because most teleosts have separate gonadotrope cell types secreting FSH and LH (Naito et al., 1991; Nozaki et al., 1990; Weltzien et al., 2003). This is in contrast to mammals, which have one gonadotrope cell type producing both hormones. Another pituitary cell type specific for teleosts are somatolactotropes (Zhu et al., 2004). The different anterior pituitary cell types of teleosts are distributed into specific areas, reflecting the initial patterning of the anterior pituitary anlage during development (Pogoda and Hammerschmidt, 2007). The RPD contains lactotropes that

produce prolactin and corticotropes that produce adrenocorticotropic hormone (ACTH), with corticotropes located dorsal to the lactotropes (Liu et al., 2003). The PPD contains thyrotropes that produce thyroid stimulating hormone (TSH) and somatotropes that produce growth hormone in the dorsal region (Herzog et al., 2003), while the ventral region mainly contains gonadotropes (Liu et al., 2003). Somatolactotropes, producing the teleost-specific somatolactin, a hormone belonging to the growth hormone/prolactin superfamily, are expressed in two different areas of the PI, one area is located at the posterior PI bordering the neurohypophysis and the other is located in the anterior part of the PI bordering the PD (Zhu et al., 2004). Melanotropes, which produces melanocyte-stimulating hormone (MSH), and some corticotropes are also located in the PI, (Liu et al., 2003).

The two different gonadotropes in teleost fish are mostly located in the PPD of the anterior pituitary. FSH and LH β-subunit transcripts have been found throughout the PPD in several species, e.g. Atlantic halibut (*Hippoglossus hippoglossus*), and the gonadotropes do not appear to be in close contact with the PN (Weltzien et al., 2003). Immunoreactivity to the LH β-subunit was found throughout the PPD, and in addition along the periphery of the PI (figure 2). Similar results have been observed in other teleosts, like Atlantic croaker (*Micropogonias undulatus*), spotted seatrout (Cynoscion nebulosus), and red drum (*Sciaenops ocellatus*), Mediterranean yellowtail (*Seriola dumerilii*) and white sea bream (*Diplodus sargus*) (Garcia-Hernandez et al., 1996; Segura-Noguera et al., 2000; Yan and Thomas, 1991). Because of the two gonadotropic cell types in teleost fish, this vertebrate class provides good model organisms for separately studying the regulation, production and secretion of FSH and LH.

1.2.3 Gonadotropins: FSH and LH

FSH and LH are part of a larger family of cysteine knot-forming polypeptide glycoproteins, which form non-covalently linked heterodimers between an α-subunit and a β-subunit. The glycoprotein tropic hormones, FSH, LH, TSH and the placenta specific chorionic gonadotropin (CG), have an identical α-subunit (glycoprotein alpha, GPA), while the β-subunit is unique to each hormone and is responsible for the biological activity. The specific FSHβ, LHβ, TSHβ, CGβ and the common α-subunit are all encoded by distinct genes (Norris, 1997; Pierce and Parsons, 1981). In addition, two recently discovered glycoproteins have been identified in some invertebrates and vertebrates, ranging from nematodes to humans. These glycoproteins are termed glycoprotein beta 5 (GPB5) and glycoprotein alpha 2

(GPA2) (Hsu et al., 2002). As these proteins are found in invertebrates it has been suggested that they represent an ancestral glycoprotein evolutionary related to the glycoproteins of the endocrine system (Roch et al., 2011). GPB5 and GPA2 are highly expressed in the hindgut of *Drosophila melanogaster* and have been suggested to function as an insect anti-diuretic hormone (Sellami et al., 2011). Moreover, GPB5 and GPA2 have also been suggested to act as a neural signaling molecule controlling intestinal function in nematodes (Oishi et al., 2009).

Upon release, FSH and LH bind to their respective receptors, FSH-R and LH-R, in the gonads, thereby stimulating gametogenesis and steroidogenesis. A large N-terminal extracellular domain responsible for the specific recognition and binding of the ligands characterizes the glycoprotein hormone receptors. In most teleost species investigated, the Lhr is highly specific for Lh, while the Fshr binds both Fsh and Lh with higher affinity for Fsh (Miwa et al., 1994; So et al., 2005; Yan et al., 1992). This differs from the situation in mammals, where the FSH and LH receptors are highly specific for their cognate hormones with few cases of cross reactivity (Braun et al., 1991; Tilly et al., 1992). The loose discrimination of gonadotrope receptors in fish could explain the potency of Lh to carry out almost all functions that are attributed to Fsh (Evans and Claiborne, 2006). Gonadotropin receptors are shown to be expressed in multiple tissues also outside the BPG axis in teleosts, for example in the gills of male Atlantic cod as well as head-kidney, muscle, stomach, heart and seminal vesicles in African catfish (Kumar et al., 2001; Mittelholzer et al., 2009; Rocha et al., 2007; So et al., 2005; Vischer and Bogerd, 2003; Wong and Van Eenennaam, 2004). This suggests that Lh and Fsh could be involved in many physiological processes although non-reproductive functions are largely unknown. The roles of Fsh and Lh during embryogenesis are not well studied, but there are some indications that Lh can have a function during the embryonic development in some species. A role of Lh in early development of fish has been suggested based on knockdown experiments in zebrafish, where increased mortality and gross abnormalities were found in morphant larvae (Chen and Chiou, 2010). However, a distinct function for LH in early embryonic development remains to be clarified.

1.3 Medaka as a research model

Medaka, *Oryzias latipes*, is a small fresh water fish, which primarily live in rice-fields in East Asia. It is a teleost with a short generation time, reaching sexual maturity within 2 to 2.5 months. The adult size is around 3 cm (Takeda and Shimada, 2010).

One reason why many fish, including medaka, are good model organisms for embryonic developmental studies is that they are oviparous, which means that the eggs develop outside the body. Medaka has several advantages as a model organism, one of them being that the eggs of medaka are transparent (Kinoshita, 2009; Takeda and Shimada, 2010). Transparent eggs make *in vivo* analysis of embryonic development possible. Medaka has a suitable breeding cycle, as they can spawn every morning when the light is turned on with a constant photoperiod. Females lay between 10 – 30 eggs each day. The eggs can develop in a wide range of temperatures, from 6 °C to 40 °C, and in low temperatures the development of the embryo slows down (Takeda and Shimada, 2010). This is convenient when performing microinjections, where the egg has to be at the one cell stage (0 – 1 hours post fertilization). The eggs can be kept on ice for 3 hours without harming the embryo.

The medaka genome is sequenced and there are several advanced techniques available to study this organism, for example the possibility to develop transgenic lines. Our group had already established a transgenic medaka line, with Gfp (which originate from sea pansy) coupled to the *lhb* promotor region. For the current project, this transgenic line was used to investigate the Gfp-*lhb* expression during medaka embryogenesis.

1.4 Embryonic development of medaka

The embryonic development of medaka is divided into 39 stages based on diagnostic features of the developing embryos (Kinoshita, 2009; for review, see Iwamatsu, 2004) . The principal diagnostic features are the number of blastomeres, the form of the blastoderm, the extent of epiboly, the development of the central nervous system (CNS), the number and form of somites, and development of different organs and other structures in the embryo (Iwamatsu, 2004). The embryonic development of medaka explained in this section is based on the work of Iwamatsu (2004) and Kinoshita et al (2009). In this paragraph, I will explain more closely some of the stages investigated in this thesis. The following text describes visual aspects of

the embryonic development, and will be helpful when discussing the results of the qualitative analysis of *lhb* expression explained later in this thesis.

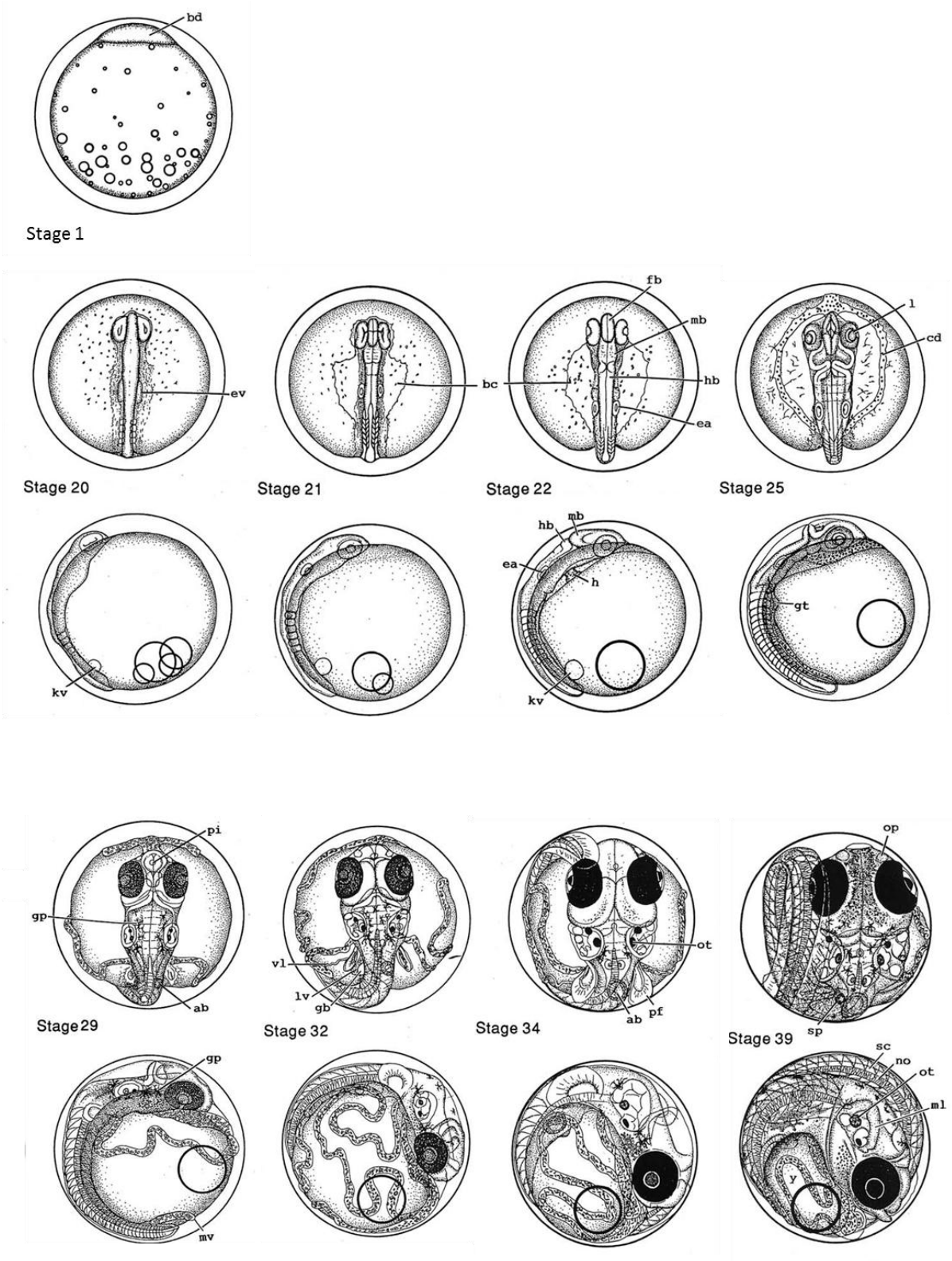

Figure 3 Selected stages of medaka development. Selected stages of medaka development shown in dorsal and lateral view. Abbreviations: ab, swim (air) bladder; bc, body cavity; bd, blastodisc; cd, Cuvierian duct; ea, otic

(ear) vesicle; ev, otic (ear) vesicle rudiment; fb, fore-brain; gb, gallbladder; gp, guanophores; gt, gut tube; hb, hind-brain; kv, Kupffer´s vesicle; l, lens; lv, liver; mb, mid-brain; ml, membrane labyrinth; mv, median yolk vein; no, notochord; op, olfactory pit; ot, otolith; pf, pectoral fin; pi, pineal gland; sc, spinal cord; sp, spleen; vl, vein of liver. Adapted from Iwamatsu (2004).

Stage 1 (0-1 hpf) One cell stage	The egg is surrounded by a thick egg envelope called the chorion. A large transparent yolk sphere is located in the center of the egg. In the animal pole the lens-shaped blastodisc is visible, and in the vegetal pole there are oil droplets in a spheric pattern.
Stage 20 (1 day, 7 h 30 min) 4 somite stage	Somites are masses of mesoderm distributed along the two sides of the neural tube that will eventually develop into muscle and the vertebral column. At this stage they are clearly distinguishable as two symmetric blocks on both sides of the embryo. A paired placode of otic (auditory) vesicles appears at the posterior region of the head. The fore-, mid- and hindbrain are now visible.
Stage 21 (1 day, 10 h) 6 somite stage	The lenses begin to form at this stage. The small otic vesicles appear, but they lack otolith. The three regions of the brain are well-defined, and the neural fold is seen as a median line along the body. The anterior region of the brain develops into the telencephalon and rostral diencephalon. The intermediate region gives rise to the caudal diencephalon, mesencephalon, and metencephalon. The posterior region develops into the myencephalon. Bilateral to the mid-brain and hind-brain, you can recognize the flat body cavity on the surface of the yolk sphere.
Stage 22 (1 day, 14 h) 9 somite stage	The heart anlage appears underneath the head from the posterior end of the mid-brain to the anterior end of the hind-brain. The body cavity extends anteriorly, incomplete lenses are present in the eyes, and the vesicular otocyst is defined.
Stage 25 (2 days, 2 h), 18-19 somite stage	This stage includes the onset of blood circulation. The otoliths appear as two structures containing small granules lying against the inner surface of each well-expanded otocyst. The embryonic body

	encircles nearly 7/12 of the yolk sphere.
Stage 29 (3 days, 2 h) 34 somite stage	The embryonic body encircles about ¾ of the yolk sphere. The structures inside the heart are differentiated. Internal ear formation occurs at this stage.
Stage 32 (4 days, 5 h) Somite completion stage	Swim bladder, kidneys and the structures inside the otic vesicles can be seen.
Stage 34 (5 days, 1 h) Pectoral fin blood circulation stage	The tip of the caudal fin reaches the eye, and the fin has developed several melanophores. The pectoral fins have blood circulation and frequently move.
Stage 39 (9 days) Hatching stage	The total length of the larvae is about 3.8 – 4.2 mm. The embryos dissolve the inner layer of the chorion, tear the single outer layer by moving the body and escape.

1.4.1 Pituitary gland formation

In all vertebrates, the pituitary gland is an organ with dual origin where the posterior pituitary derives from the neuroectoderm and the anterior pituitary derives from non-neural tissue (Zhu et al., 2007). The initial steps of anterior pituitary formation in vertebrate species can be traced back to early segmentation stages, which start shortly after the completion of gastrulation (Pogoda and Hammerschmidt, 2009). In mammals, the pituitary develops through a fusion of two tissues (figure 4). In early gestation in mammals, a finger of ectoderm grows upward from the roof of the mouth. This protrusion is called Rathke's pouch and will develop into the anterior pituitary. This invagination of Rathke's pouch towards the diencephalon (the separation of the pouch from the oral ectoderm) marks the first detectable expression of a pituitary preprohormone, proopiomelanocortin (pomc), in mouse and rat (Begeot et al., 1982; for review, see Kioussi et al., 1999). Pomc is a precursor for several derivatives, including ACTH and α-MSH. At the same time as Rathke's pouch is developing, another finger of ectodermal tissue, the infundibulum, evaginates ventrally from the diencephalon of the

developing brain. This extension of the ventral brain will become the posterior pituitary (Norris, 1997).

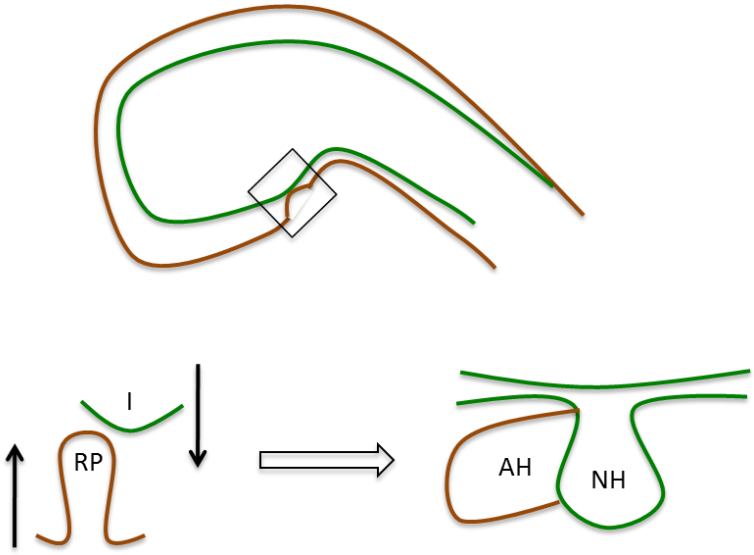

Figure 4 Pituitary development in mammals. This figure shows a representation of the interaction between the infundibulum (I) and Rathke's pouch (RP). The infundibulum extends down from the developing brain and contacts Rathke's pouch from the embryonic pharynx. Rathke's pouch will develop into the non-neural anterior pituitary (adenohypophysis, AH) and the infundibulum will develop into the posterior pituitary (neurohypophysis, NH).

In zebrafish, however, after the completion of gastrulation the neural plate is bordered by the preplacodal ectoderm (ppe) rostrally and the neural crest caudally. The anterior pituitary cells (together with various other cell types) derive from the ppe. The cells here are arranged in a specific spatial pattern, and the most anterior domain of the ppe (the anterior neural ridge) contains the future anterior pituitary cells (Pogoda and Hammerschmidt, 2009). The posterior pituitary derives from the ventral diencephalon (Pogoda and Hammerschmidt, 2007). There are no invagination equivalent to Rathke's pouch formation in zebrafish (Herzog et al., 2003). Instead, pituitary cells, which are distributed in a horseshoe-like pattern, move inwards together with precursor cells of the mouth during oral cavity formation, with medial cells of the placode ending up posteriorly and lateral cells ending up anteriorly, resulting in an anterior-posterior, rather than dorsoventral, patterning of the anterior pituitary (Herzog et al., 2003). Moreover, there are evidence showing the differentiation of *pomc* and *prolactin* expressing pituitary cell types in zebrafish prior to any inward movement that could be equivalent to Rathke's pouch formation (Herzog et al., 2003; Liu et al., 2008).

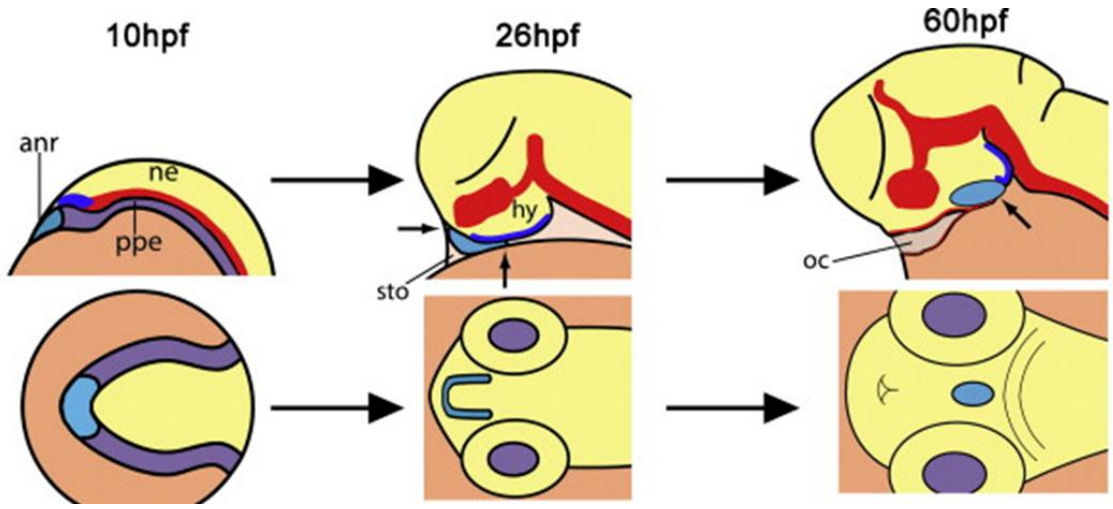

Figure 5 Development of the zebrafish anterior pituitary. The first row shows lateral views of the headregions of embryos and larvae at different developmental stages. The second row shows dorsal views of the zebrafish embryo and larvae. The anterior pituitary is shown in light blue, yellow color indicates the neural ectoderm (ne) and the preplacodal ectoderm (ppe) is shown in purple. Adapted from Podoga and Hammerschmidt (2009).

The patterning of the pituitary anlage and terminal differentiation of pituitary cells in zebrafish start while cells are still organized in a placodal fashion at the anterior edge of the developing brain in early segmentation stages (Herzog et al., 2003). In zebrafish, the lactotropes, somatolactotropes and corticotropes differentiate and start expression of their respective hormone genes prolactin, somatolactin and pomc before anterior pituitary internalization is initiated (Herzog et al., 2003; Lopez et al., 2006). At the onset of anterior pituitary internalization, the anterior pituitary anlage has acquired a horseshoe-like shape, lining the anterior and lateral borders of the ventral diencephalon (Herzog et al., 2004; Liu et al., 2008; Pogoda and Hammerschmidt, 2007). The anterior pituitary lies between the ventral diencephalon and the dorsal roof of the mouth and as it gets pressed between these two structures, it becomes progressively shifted posterior-wards (figure 5). At this time of development *gpa* and *tsh* can be detected (Herzog et al., 2003). However, the β-subunits of Fsh and Lh, which gives the gonadotropins their specific biological activity, have been detected in the embryonic stages, but the tissue specificity is unknown (Nica et al.,2006). The distinct pituitary cell lineages display a specific pattern along the anterior-posterior axis of the gland when the anterior pituitary has reached its final position in the developing larva (Pogoda and Hammerschmidt, 2007).

1.4.2 Gut tube formation

While investigating the tg(*lhb*:GFP) medaka line, it became evident that the *lhb* expressing cells were not located in the pituitary (see Results). Therefore, other tissues located in the area of the Gfp expressing cells needed to be investigated in more detail. The gut endoderm is the site of nutritional digestion and absorption and has an essential function in embryonic development by providing the anlage and signals to form the many endoderm derived organs such as thyroid, liver and pancreas (Kobayashi et al., 2006). The digestive system and its development are extensively studied in amniotes (for a review, see Grapin-Botton and Melton, 2000). Wells and Melton (1999) compared the gut tube formation in frog (Keller, 1975), chick (Rosenquist, 1971), and mouse (Lawson and Pedersen, 1987) and found that the process of gut tube formation is highly conserved in many vertebrates. The gut formation consists of two invaginations of the endodermal sheet, one at the anterior end to form the foregut, followed by a posterior invagination to form the hindgut (Wells and Melton, 1999). Now, the mesoderm consists of two layers. The inner layer, the splanchnic mesoderm, is closely associated with the endoderm and undergoes muscle differentiation around the endoderm. Later in the developmental phase, there is an axial growth of the foregut and hindgut from the intervening endoderm. At the same time, morphogenesis of the midgut takes place. This process completes the formation of the continuous gut tube (Wells and Melton, 1999).

There are, however, some differences in gut tube formation when it comes to fish. In zebrafish, the most anterior domain that will develop into the pharynx and esophagus develops separately from the more posterior domains of the gut tube. In amniotes, the anlagen of the pharynx, esophagus and intestine primordial arise from the foregut. Whereas gut tube formation in amniotes involves folding of an endodermal sheet, the zebrafish gut tube formation involves rearrangement of newly polarized cells (Wallace and Pack, 2003). This suggests that there are some unique differences in gut tube formation in terms of morphogenesis between species, even though many genetic factors seem to be conserved (Kobayashi et al., 2006).

In medaka, as in zebrafish, the anterior part of the endodermal sheet gives rise to the pharynx and esophagus and the remaining part of the endodermal sheet gives rise to the intestine. The part that gives rise to the intestine is called the gut tube. The gut tube can further be divided into the rostral, intermediate and caudal portions (Kobayashi et al., 2006).

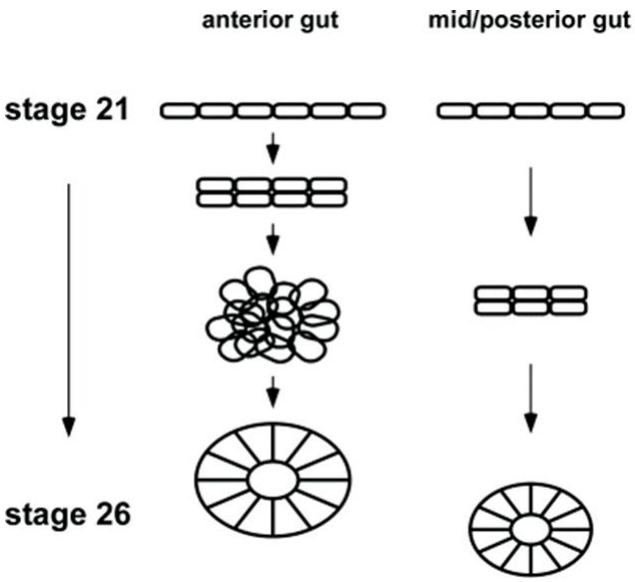

Figure 6 A schematic representation of the gut tube formation in medaka. The gut tube formation starts by generating a bilayer at stage 22 in the anterior portion of the endoderm. The development of the gut tube is finished when the lumen of the gut is finally visible in the caudal region at stage 26. From Kobayashi et al. (2006).

Before the gut tube formation starts (stage 21, 34 hpf), the endodermal sheet is a monolayer of cells located ventral in the larvae (figure 6). The gut tube formation is initiated when the rostral part of the endoderm starts to migrate towards the midline, to form a cell aggregate, in the rostral portion of the gut tube. This cell aggregate forms a dorso-ventrally flattened bilayer of cells, while the cells in the caudal portion still maintains as a monolayer. The rostral portion of the gut tube now forms a rod-like structure but the lumen is still not visible. The rostral portion starts to show a radial organization, with nuclei on the basal side, at stage 24 (44 hpf) and this is the same time as the liver bud is observed for the first time, positioned slightly left of the midline. When the lumen is visible for the first time in the rostral portion of the gut tube, the cells in the caudal portion starts to migrate towards the midline. The development of the gut tube gradually expands posteriorly to finally reaching the caudal end, the cloaca, at stage 26 (54 hpf). The gut tube formation is finished when the most caudal part finally acquires a lumen (Kobayashi et al., 2006).

1.5 Generation of transgenic lines

Transgenesis is the process by which an exogenous gene can be introduced into an organism, enabling the organism to express a new gene and, if the gene gets incorporated into the germline, transmit that gene to its offspring. By increasing the magnitude of gene expression (for example with an extra copy controlled by a strong promotor) or by introducing a reporter gene downstream an endogenous promotor sequence, it is possible to study the expression and function of genes. Transgenic organisms are, therefore, powerful tools for elucitading gene function. There are several methods to facilitate transgenesis and two of these methods will be described in this thesis; the bacterial artificial chromosome (BAC) method (described in section 2.3) and plasmid-based transgenesis with meganuclease technology. When the BAC method is utilized, a BAC containing the gene of interest is selected. These are readily available for many species as there are existing libraries where BACs are generated for genomes sequencing projects and you can find a BAC containing the gene of interest. A BAC is much bigger than a conventional plasmid and could contain all the distal regulatory sequences of the gene of interest, depending on its location in the BAC. The inclusion of major regulatory elements would minimize the chance of having ectopic expression. When generating a reporter construct with a BAC, a fluorescent protein is inserted downstream of the promotor region of the gene of interest. On the other hand, when performing a conventional plasmid-based transgenesis to generate a reporter construct, both the promotor region of the gene of interest and a fluorescent protein needs to be ligated into a vector. In this method, the distal regulatory sequences of the promotor region will not necessarily be present in the vector. This could have an effect on the transcription of the gene of interest in the organism. In this thesis, a vector with meganuclease sites on either side of the transgenic insert was used. The integration of a transgene into the genome is easier with smaller constructs and meganuclease sites are reported to facilitate the integration of transgenic constructs into the medaka genome (Rembold et al., 2006; Thermes et al., 2002). In this way, the integration of a transgene (cut out with meganuclease enzyme) is expected to be integrated with higher efficiency than a BAC construct. However, the larger portion of a promotor region in a BAC construct may improve the specificity of the transgenic construct after integration.

1.6 Aims of this study

In my thesis, a characterization of an already established transgenic medaka line was performed. To get a comprehensive structure of the technical experience in my thesis we wanted to include the generation of another transgenic construct and development of a second transgenic line. This will also help the overall scientific aims of my research group. The aims of my thesis are therefore:

1. Characterization of the spatial and temporal *lhb* gene expression during medaka embryonic development to clarify the possible function of this hormone during development.

2. Generation of a tg(*fshb*:RFP) construct and a stable transgenic medaka line for subsequent characterization of *fshb* gene expression during medaka embryonic development.

2 Materials and methods

In this thesis, a tg(*lhb*:GFP) line (Gfp, downstream of the *lhb* promotor) was used for qualitative and quantitative analysis of the *lhb* expression in embryos. Since our lab had already established the tg(*lhb*:GFP) line, generation of a new transgenic line with red fluorescent protein (Rfp) coupled to the *fshb* promotor (*fshb*:RFP) was also included to complement the overall aims of this thesis. A methodological overview of this master thesis is shown in figure 7.

The *in situ* hybridization (ISH) experiments explained in this thesis were performed by another member of my group, Jon Hildahl. The experiments were included because they provide further evidence that Gfp-*lhb* was expressed outside the developing pituitary during embryogenesis.

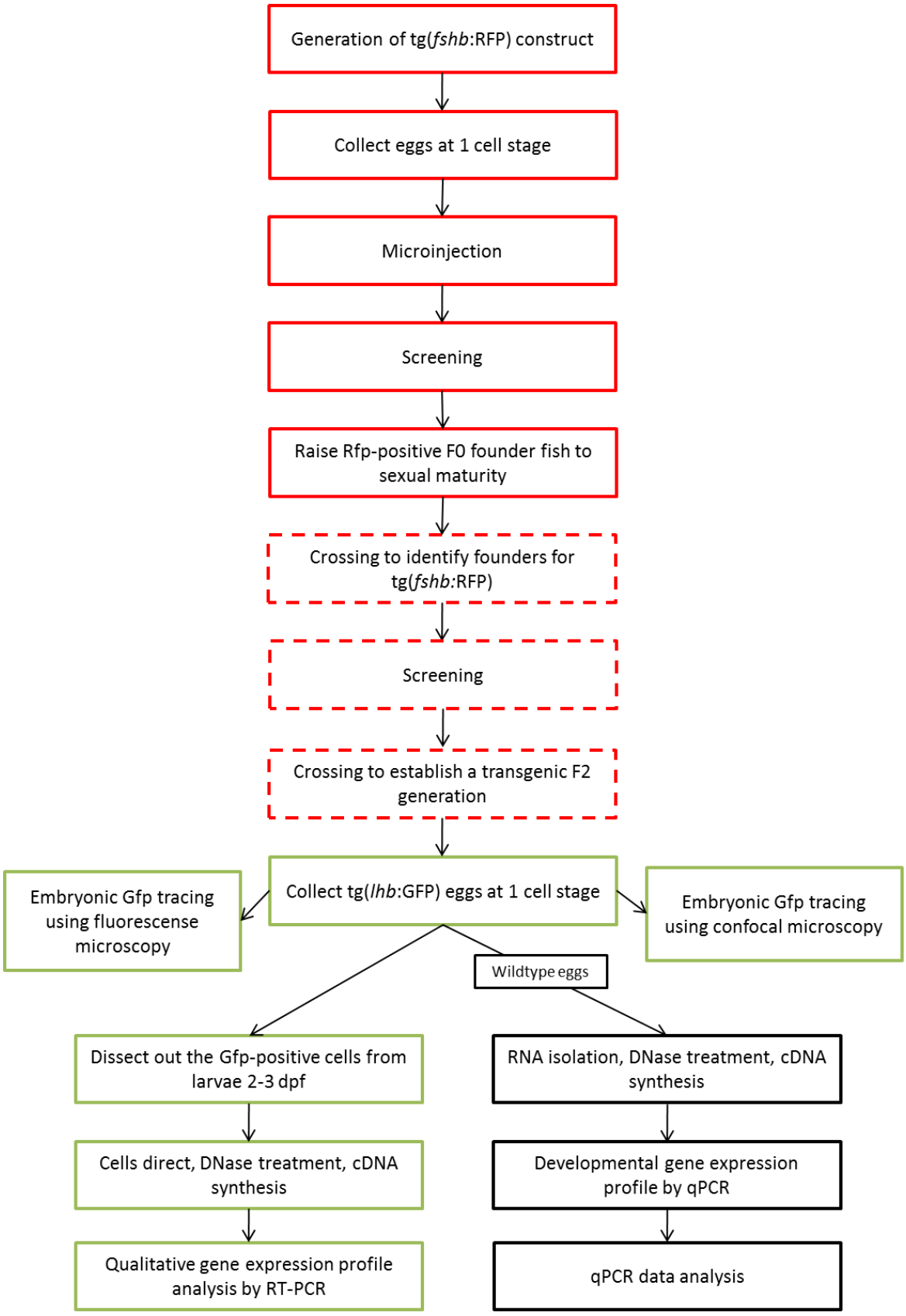

Figure 7 Overview of the methodological approach used in this master thesis. Experiments to generate the tg(*fshb*:RFP) line is marked in red, while analysis of the tg(*lhb*:GFP) line is marked in green. Black indicates experiments where wildtype fish were used.

2.1 Generation of the tg(*fshb*:RFP) construct

To establish a fluorescent reporter transgenic line, a vector containing a fluorescent protein sequence downstream of a target gene promotor, needed to be generated (figure 8). As mentioned earlier, different methods can be utilized to generate such a transgenic construct. The BAC homologous recombination technology (Nakamura et al., 2008) was applied in attempts to generate a tg(*fshb*:GFP) line, but we could not identify any positive fish in the F_0 generation nor F_1 generation. Instead, a plasmid-based construct with meganuclease technology was generated. A PCR reaction with genomic DNA from medaka as template and *fshb* primers was used to produce a *fshb* promotor insert. After restriction enzyme digestion of the *fshb* insert and the *rfp* vector, the *fshb* insert was ligated into the corresponding restriction sites of the pBluescript II SK vector. The vector then contained the *fshb* promotor upstream of the *rfp* sequence. After several controls (described in sections 2.1.8 – 2.1.10), the construct was microinjected into one cell stage medaka embryos. The meganuclease sites on both sides of the transgene would cut the transgene out of the vector and mediate a more efficient incorporation into the genome. When incorporated into the genome, Rfp was expected to be expressed in the same cells and at the same time as endogenous *fshb*.

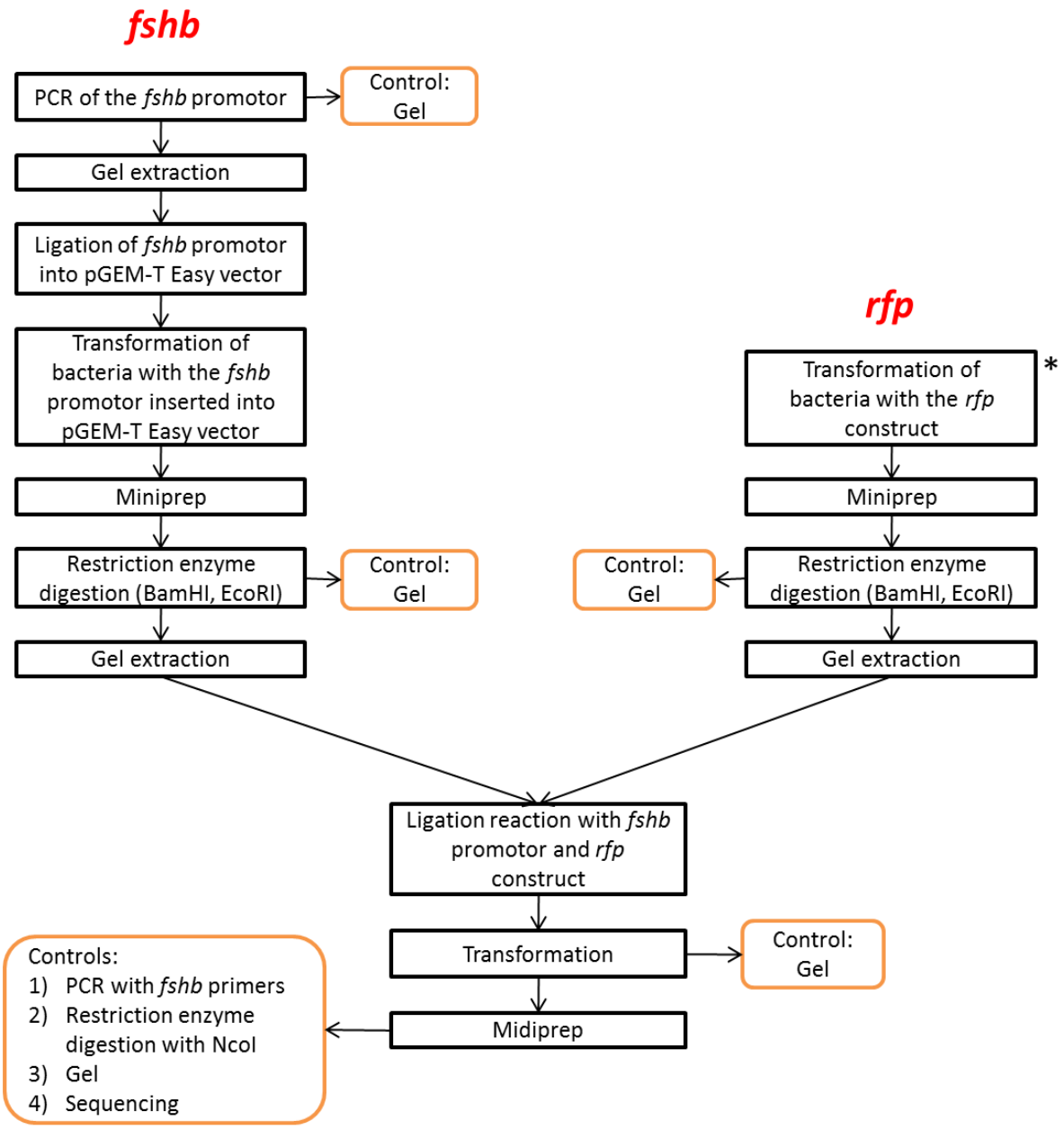

Figure 8 Overview of the methodological approach used in the generation of the tg(*fshb*:RFP) construct. The methodological steps in this figure are described in detail in the next sections. * A pBluescript II SK vector containing *rfp* insert and meganuclease cut sites was kindly provided by Dr. Christoph Winkler at The National University of Singapore. It is the mCherry sequence ligated into a pBluescript vector. We received the sample as a miniprep.

2.1.1 PCR of the *fshb* promotor

The *fshb* promotor sequence, exon 1, intron 1 and the first part of exon 2 just upstream the endogenous start site (see figure 9 A) were PCR amplified using AccuPrime Taq DNA polymerase high fidelity (Invitrogen, Carlsbad, CA, USA), with 105 ng of medaka genomic

DNA (21 ng/µl) as template for each reaction. Two different primer pairs for *fshb* were used (fshbF1+fshbR for the long promotor sequence and fshbF2+fshbR for the short promotor sequence, see table 1), with expected PCR product lengths of 4000 and 2500 bp, respectively. The two different lengths of the promotor region were used because we wanted to include as much promotor as possible, but the integration into the genome is more efficient with smaller inserts. The reverse primer used in the PCR reactions was the same for both *fshb* inserts and integrated a BamHI cut site in the 3´-end of the *fshb* sequence. The forward primers were different, with an EcoRI cut site integrated in the forward primer sequence for the short (2500 bp) *fshb* insert, while an endogenous EcoRI cut site was identified just downstream of the forward primer sequence in the long (4000 bp) *fshb* sequence.

Table 1 Primer list

Primer	Genes	Application	Primer sequences
bactF	*bactin*	co-localization	5´-ACCCTGTCCTGCTCACTGAA-3´
bactR	*bactin*	co-localization	5´-GCAGGGCTGTTGAAAGTCTC-3´
lhbF1	*lhb*	qPCR	5´-CCACTGCCTTACCAAGGACC-3
lhbF2	*lhb*	co-localization	5´-CACAGCCTGCAGATACATGAG-3'
lhbR	*lhb*	co-localization, qPCR	5´-AGGAAGCTCAAATGTCTTGTAG-3´
fshbF1	*fshb*	generate long tg(*fshb*:RFP)	5´-CCCAGTGTTAAGGTTTCAGA-3´
fshbF2	*fshb*	generate short tg(*fshb*:RFP)	5´-GAATTCGCCTCTGTAAATGAATGTG-3´
fshbF3	*fshb*	sequencing of tg(*fshb*:RFP) construct	5´-TCAAGCTCATGTTCTAAAGTGATGT-3´
fshbR	*fshb*	generate tg(*fshb*:RFP)	5´-GGATCCCCTCTGCCTGGTGCAGT-3´
gfpF	*gfp*	co-localization	5´-GTGAGCAAGCAGATCCTGAAG-´3
gfpR	*gfp*	co-localization	5´-TACTTGGTGAAGGTGCGGTTG-´3
lhx3F	*lhx3*	co-localization	5´-CTAGAACATCCGGGCTCA-´3
lhx3R	*lhx3*	co-localization	5´-ATCTAACCAGGACGCAGGA-´3
16sF	*16s*	qPCR	5´-CGATCAACGGACCGAGTTACC-3´
16sR	*16s*	qPCR	5´-AATAGCGGCTGCACCATTAGG-3´

Molecular grade water was mixed with 5 µl 10X AccuPrime Buffer II, 1µl sense primer (10 µM), 1 µl antisense primer (10 µM), 5 µl template DNA and 1 µl Accuprime Taq high fidelity to a final volume of 50 µl. The PCR reaction was performed on a thermal cycler (Mastercycler gradient, Eppendorf, Hamburg, Germany) with the following cycling parameters: 94 °C for 2 min; 30 cycles of 94 °C for 30 sec, a gradient on the heat block of 45 – 55 °C for 30 sec, 68 °C for 4 min; followed by an additional elongation step at 68 °C for 10

min. A gradient was used in the annealing step because the two different primer pairs had melting temperatures of 54.2 and 52.0 °C, respectively. By using a gradient, several PCR reactions were performed simultaneously. The PCR products were run on a 1% agarose gel to verify the product size (for gel picture, see results) and as a first step to purify the correct PCR product by gel extraction.

2.1.2 Gel extraction

Gel extraction was performed following the QIAquick Gel Extraction Kit Protocol (Qiagen, Hilden, Germany). The chosen DNA fragment was excised from the gel, the weight measured and 3 volumes of Buffer QG added to dissolve the gel. This process was enhanced by incubation at 50 ºC for 10 min. To increase the yield of DNA fragments, one gel volume of isopropanol was added to the sample. The sample was transferred to a QIAquick column that binds DNA before centrifuged using a Kubota 3500 centrifuge (Kubota, Tokyo, Japan) at 10,000 g for 1 min. Buffer QG was added to remove all traces of agarose, then Buffer PE to wash the DNA with a 1 min centrifugation (10,000 g) following each step. The flow-through was discarded and the sample centrifuged at 10,000 g for 1 min to completely dry the membrane. By adding 30 µl elution buffer to the membrane then centrifuge for 1 min, DNA was eluted.

2.1.3 Ligation

Ligation of *fshb* promotor into pGEM-T Easy vector was performed according to the manufacturer's protocol (Promega, Madison, WI, USA). Five µl 2x rapid ligation buffer, 1 µl pGEM-T Easy vector (50 ng), 1 µl T4 DNA ligase and 3 µl of *fshb* PCR product were mixed before incubation at room temperature for 1 hour, followed by incubation at 4 °C overnight to increase ligation efficiency.

Ligation of the *fshb* PCR product into pBluescript II SK vector (containing the *rfp* insert) used the same components as the ligation reaction described above, however, the amount (ng) of *fshb* promotor insert and pBluescript II SK vector/*rfp* was calculated from the following equation:

Equation 1

$$\frac{\text{ng vector} \bullet \text{insert bp}}{\text{vector bp}} \bullet 3 = \text{ng insert}$$

The reaction was incubated at room temperature for 1 hour, followed by incubation at 4 °C overnight to increase ligation efficiency.

2.1.4 Transformation

Three different transformation reactions were carried out when generating the tg(*fshb*:RFP) construct. First, a transformation with the *fshb* promotor inserted in pGEM-T Easy vector was performed. Second, the construct with an *rfp* sequence ligated into a pBluescript II SK vector was provided as a miniprep sample and a transformation reaction was performed to increase the amount of construct. Third, a transformation reaction was carried out after ligation of *fshb* insert into the *rfp* (pBluescript II SK) vector.

Transformation reactions were performed following the manufacturer's protocol (Promega). When transformation was done with the pBluescript II SK/*rfp* miniprep or after the *fshb* ligation reaction, 1 µl or 3 µl of the sample was used, respectively. To a tube containing DNA of interest, 50 µl of JM109 High Efficiency competent cells (>108 cfu/µg) (Promega) was added. The sample was placed on ice for 20 min then heat-shocked at 42 °C for 45-50 sec. Following 2 min on ice, 950 µl of Super Optimal Broth with Catabolite repression (SOC) medium was added to the reaction and the tube incubated at 37 ºC for 1.5 hours with shaking. The transformation culture was plated out on two different selective LB/Ampicillin/IPTG/X-Gal plates with different volumes (25 µl and 50 µl) before incubation overnight at 37 ºC. Blue/white color selection was used to eliminate cultures where the insert were not present. The *lacZ* gene is coded in the multiple cloning site (MCS) of the plasmid. If an insert disrupts this gene, there will not be generated any β-galactosidase, thus the colony will have a white color. If β-galactosidase is made, the colony will be blue and the insert will not be present in the plasmids of the colony.

2.1.5 Miniprep

Plasmid DNA purification was performed according to the manufacturer's protocol (QIAGEN Plasmid Mini Kit, Qiagen). From the selective agar plates, a single white colony was picked then incubated in 3 ml LB medium with ampicillin for 16 hours at 37 ºC with vigorous shaking. The bacterial cells were harvested by centrifugation (Beckman Coulter Allegra X-22R centrifuge) at 6000 g for 15 min at 4 ºC. Addition of 300 µl Buffer P1 would re-suspend the bacterial pellet. To lyse the bacterial cells, Buffer P2 was added and the tube inverted until the suspension was homogenous. The sample was incubated at room temperature for 5 min. Chilled Buffer P3 was added to precipitate the genomic DNA (gDNA), proteins, cell debris and potassium dodecyl sulfate (KDS). The solution was mixed by inverting the tube, then incubated on ice for 5 min. Cold buffer and incubation on ice enhanced the precipitation process. Centrifugation at 18,000 g for 10 min was used to pellet the precipitate, before removing the supernatant containing the plasmid DNA. A QIAGEN-tip 20 column was equilibrated by applying Buffer QBT, followed by addition of the supernatant containing plasmid DNA. The column was washed with Buffer QC and DNA eluted with Buffer QF. The DNA was precipitated by adding 0.7 volume of isopropanol, whereupon the sample was mixed and centrifuged at 18,000 g for 30 min. After centrifugation the supernatant was removed then the DNA pellet washed with 70 % ethanol and centrifuged at 18,000 g for 10 min. The 70% ethanol removes precipitated salt and replaces isopropanol with the more volatile ethanol, making the DNA easier to re-dissolve. The pellet was air-dried and then re-dissolved in 50 µl nuclease-free water (Ambion). The amount of DNA extracted was measured with NanoDrop spectrophotometer (Thermo Fisher scientific, USA).

2.1.6 Restriction enzyme digestion

Both pBluescript II SK with *rfp* insert (restriction sites shown in figure 9B, pBluescript vector shown in figure 9C) and pGEM-T Easy vector with *fshb* promotor insert were cut with two restriction enzymes, EcoRI and BamHI. A reaction mix with 2 µl 10x REACT 3 buffer, 1 µl EcoRI, 1 µl BamHI, 1 µg vector and dH2O up to 20 µl was prepared then the reaction incubated at 37 °C for 1.5 hours before being inactivated by incubation at 65 °C for 15 min.

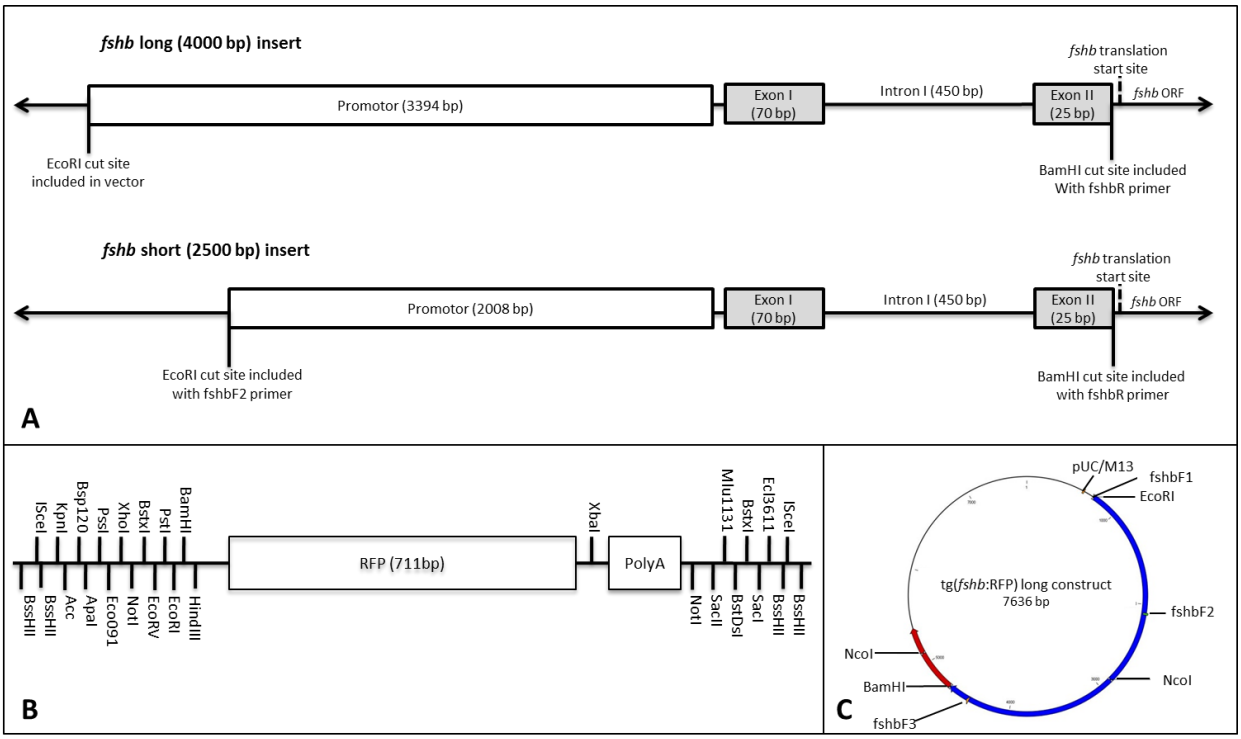

Figure 9 Sequences and vector included in the tg(*fshb*:RFP) construct. A) Representation of the long and short *fshb* sequences generated from the PCR reaction. EcoRI and BamHI are the restriction enzymes used to cut out the *fshb* sequence from gDNA used to generate the construct from the endogenous *fshb* sequence. *fshb* translation start site is not included in the sequence used for the construct, hence the *rfp* translation start site will be used instead. ORF: open reading frame. B) Cut sites in the pBluescript II SK vector and the *rfp* sequence. The *fshb* sequence was ligated into the vector upstream of the *rfp* sequence between EcoRI and BamHI restriction sites. C) Schematic representation of the pBluescript SK II+ vector with *rfp* (red) and long *fshb* sequence (blue) included. Primers for sequencing (pUC/M13 and fshbF3) are shown. The primer named fshbF2 shows where the short *fshb* sequence starts. Restriction enzyme cut sites for NcoI, BamHI and EcoRI are also shown in the representation.

2.1.7 Midiprep

Plasmid purification was performed according to the manufacturer's protocol (QIAGEN Plasmid Midi and Maxi Kits, Qiagen). One colony from a blue/white selective plate and 5 ml LB medium with ampicillin (50 µg/µl) was incubated for 8 hours at 37 °C with vigorous shaking (300 rpm). This liquid culture was diluted 1/500 into fresh selective LB medium then set to grow at 37 °C for 16 hours with vigorous shaking. The bacterial cells were harvested by centrifugation at 6000 g for 15 min at 4 °C, before the pellet was re-suspended in a re-suspension buffer containing RNase A. Next, lysis buffer was added and the suspension mixed by inverting the tube several times followed by incubation at room temperature for 5

min. The addition of cold neutralization buffer would precipitate gDNA. After vigorous shaking, the tube was incubated on ice for 15 min to enhance precipitation. The cell suspension was then centrifuged, before the supernatant containing plasmid DNA was removed. A Qiagen-tip 100 column was equilibrated using the equilibration buffer QBT, and the supernatant applied to the column. After the supernatant had entered the resin, the column was washed two times with wash buffer QC, then DNA eluted by applying the elution buffer QF. DNA was precipitated by adding 0.7 volumes of isopropanol and centrifuged at 15,000 g for 30 min at 4 °C. The pellet was washed with 70% ethanol then centrifuged at 15,000 g for 10 min. After centrifugation ethanol was removed and the pellet air-dried. The pellet was re-dissolved in 50 µl TE buffer.

2.1.8 Control: PCR with *fshb* primers

A PCR reaction with the tg(*fshb*:RFP) constructs as template and *fshb* primers were done to confirm the incorporation of *fshb* insert into the vector. The PCR reactions using AccuPrime Taq high fidelity polymerase (Invitrogen) were run on a thermal cycler (Mastercycler gradient, Eppendorf) with the parameters described in section 2.1.1.

2.1.9 Control: Restriction enzyme digestion with NcoI

An additional control of the tg(*fshb*:RFP) construct was carried out by performing a restriction enzyme digestion with the restriction enzyme NcoI. Molecular grade water was mixed with 2 µl NEBuffer 3, 1 µl NcoI enzyme, 1 µg of midiprep reaction to a final volume of 20 µl and incubated for 1 hour at 37 °C. NcoI had restriction sites inside the *fshb* and *rfp* sequences. If both genes were incorporated into the vector, this analysis would give two bands on the 1% agarose gel, whereas if the insert was missing, only one band would appear on the gel.

2.1.10 Control: Sequencing

To further confirm that the tg(*fshb*:RFP) construct contained both the *rfp* and the *fshb* sequence, the 3' and 5' ends of *fshb* and *rfp* were sequenced. Nuclease-free water (Ambion) was mixed with 1 µl plasmid DNA (400 – 600 ng/µl) and 3.5 µl of forward primer pUC/M13 (Promega, 10 µg/ml) or 2 µl of *fshb* forward primer (5µM) to a final volume of 10 µl was used in the sequencing reaction. The pUC/M13 primer (Promega) started upstream of the *fshb*

sequence and the forward primer for *fshb* started in the 5`end of the *fshb* sequence. The samples were sequenced at the ABI-lab at the University of Oslo.

2.2 Generation of a stable tg(*fshb*:RFP) medaka line

2.2.1 Animal handling

Japanese medaka *(Oryzias latipes*, d-rR strain*)* were kept in the aquarium facilities at the Department of Molecular Biosciences, University of Oslo. The fish were maintained in water recirculating systems equipped with particle and charcoal filters, a UV-lamp and a biofilter to maintain water quality (Marine Biotech, FL, USA). To promote spawning, the photoperiod was adjusted to a 14-hour light 10-hour dark cycle, and the water temperature kept at 27 °C. System water was produced from pre-filtered tap water (20 and 5 μm particle filters, charcoal filter) followed by reverse osmosis. The purified water was added the following salts per 100 l: marine salt (20 g, Seachem, Madison, GA, USA), $CaCl_2$ (1.5 g) and $NaCO_3$ (5 g), resulting in a system water conductivity of 380 – 420 μS and pH of 7.3 – 7.8. The water in the racks displayed conductivity of 440 – 490 μS and pH of 6.8 – 7.5. About 20% of the water in the fish racks was renewed with fresh system water daily. The fish were fed two to five times per day with newly hatched brine shrimp nauplii *(Artemia salina)* (Argent Chemical Laboratories, Redmond, WA USA) and dry feed (Scientific fish food, Special Diets Services, Essex, UK).

2.2.2 Microinjection of the construct

The needles used for microinjection were made from borosilicate GD-1 glass capillaries (Narishige, Tokyo, Japan) which had an outer diameter of 1.0 mm. Glass needles were made using a vertical needle puller Model PC-10 (Narishige). To optimize the tip of the needle for injection, Micro Grinder EG-400 (Narishige) was used. To bevel the tip, the needle and the grinder formed a 30-degree angle then the tip of the needle was carefully lowered to the grinder by using a micromanipulator (Narishige). To control the width of the opening, air pressure was applied when the tip was under water and the width estimated from the size of the air bubbles.

Eggs were collected just after the lights were turned on in the morning. Light initiates spawning, so the majority of eggs are at one cell stage at this time. Females carry their eggs

after spawning, and the eggs were collected directly from the abdomen of the fish then immediately placed in E3 medium (5 mM NaCl, 0.17 mM KCl, 0.33 mM $CaCl_2$, 0.33 mM $MgSO_4$ and methylene blue) on ice, until visual inspection under a dissecting microscope. The low temperature arrests the development of the embryo. We were only interested in eggs that had progressed to one cell stage to avoid mosaic distribution of the construct. One cell stage is reached 0-1 hours post fertilization (hpf) at 27 °C. Eggs that had progressed beyond one cell stage were discarded.

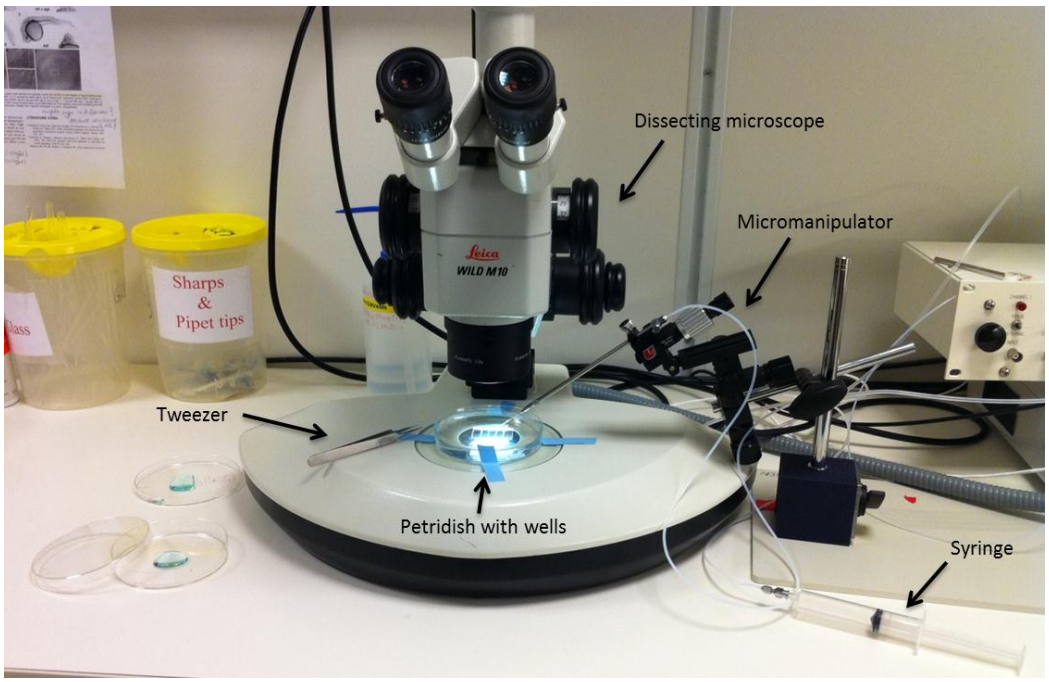

Figure 10 Materials used for microinjection. Dissecting microscope, micromanipulator, syringe, fine tweezers and petri dish with wells.

To stabilize the eggs during the microinjection, a petri dish containing a glass plate with wells of 1 mm was used. The petri dish was filled with 1x phosphate buffered saline (PBS: 137 mM NaCl, 2.7 mM KCl, 4.3 mM Na_2HPO_4, 1.47 mM KH_2PO_4, pH 7.4) and the eggs placed in the wells. A fine tweezer was used to manipulate the eggs. Microinjection was performed under a stereomicroscope and the needle insertion controlled by a micromanipulator (GJ-1 magnetic base, Tritech research, CA, USA). The needle was also coupled to a disposable syringe through a silicone tube such that when pressure was applied, the content was released (figure 10). The appropriate injection volume should be about the same size as the oil droplets in the yolk sac, about 0.5 – 1 nl (figure 11).

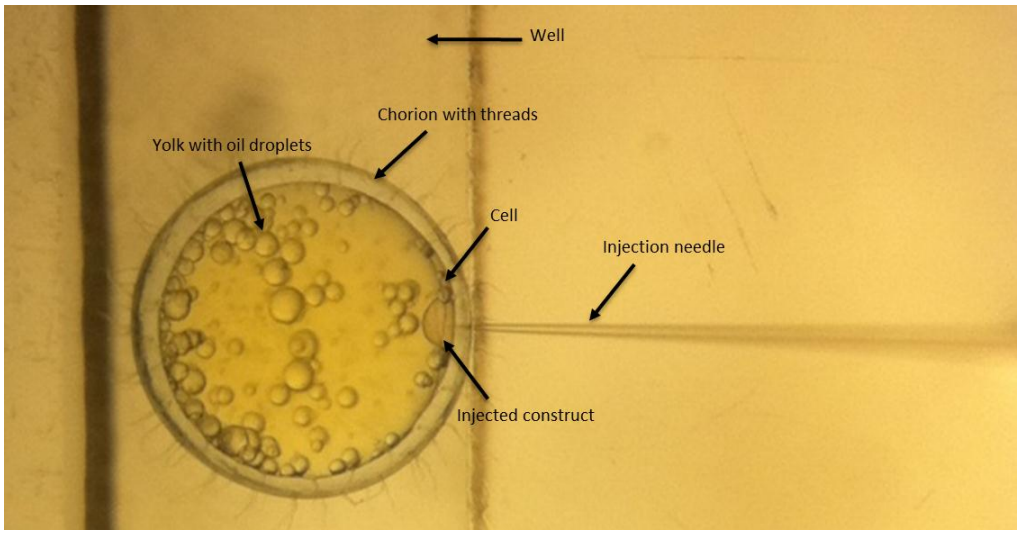

Figure 11 Microinjection of tg(*fshb*:RFP) construct. The volume injected should be similar to the largest oil droplets in the egg.

The two different tg(*fshb*:RFP) constructs were injected with a concentration of 2 – 3 ng/µl. A high concentration that does not induce high mortality was used to ensure an enhanced success rate. To determine if the concentration of the construct was suitable, the death rate had to be controlled and should not exceed 50 %. The construct was diluted in 1 x PBS and 1:20 phenol red added to the mix for visualization of the injection volume. Injected DNA persists as long extra-chromosomal concatamers transiently transcribed during early embryogenesis. Mosaic expression is when the transgene is only seen in some of the somatic cells, which is often the situation in the F_0 generation due to an uneven distribution of this episomal DNA (Thermes et al., 2002).

Both constructs were also injected after treatment with the meganuclease *I-SceI*. The transgene of interest (*rfp-fshb*) was flanked by *I-SceI* meganuclease recognition sites and when pretreated with this enzyme, a 30 % higher transgenesis frequency was expected (Thermes et al., 2002). The meganuclease *I-SceI* will statistically cleave randomly only once in 7 x 10^{10} bp (Thermes et al., 2002), and will therefore not cut the host genome randomly. The meganuclease will cut the transgene out of the vector and thereby mediate efficient integration. To 27 µl of the preferred concentration of construct, 1.5 µl of *I-SceI* enzyme and 1.5 µl NE Buffer 1 was added, followed by incubation at room temperature for 1 hour. After incubation, the construct could be kept on ice for 3 hours while the injection was performed. As a control for egg quality, 10 eggs were collected from the same batch as the microinjected eggs and the death rate was registered.

2.2.3 Screening

The microinjected eggs were screened every day from 2 days post fertilization (dpf), until 5 dpf. The screening process began at 2 dpf because a pilot quantitative PCR (qPCR) experiment with *fshb* primers indicated that the *fshb* gene expression starts around 48 hours post fertilization (hpf).

2.2.4 Breeding and raising a homozygous tg(*fshb*:RFP) medaka line

The microinjected eggs were incubated at 27 °C until hatching and grown to sexual maturity (expected January 2012) in regular fish tanks. The fish injected with different constructs were kept separated. When the fish become sexually mature, they will be crossed with each other to identify the founder fish for the tg(*fshb*:RFP) construct. All the microinjected eggs will be crossed even though they did not show any fluorescence in the first screening process. This is because the mosaic expression can make it hard to detect the *fshb* expressing cells in the F_0 generation.

2.3 Generation of the tg(*lhb*:GFP) construct

The tg(*lhb*:GFP) and tg(*fshb*:RFP) (described in section 2.1) constructs were generated using different transgene technologies. The BAC homologous recombination technology (Nakamura et al., 2008) applied by other members of our group to generate the tg(*lhb*:GFP) construct, successfully produced a stable transgenic line (submitted, Hildahl et. al. 2011). Thus, I also tested the BAC method to produce a tg(fshb:GFP) line without success. By performing an *in silico* search (http://medaka.utgenome.org/) a BAC clone containing the gene of interest (*lhb*), BAC golwb_108_H20, which contains approximately 25 kb 5'-flanking region and approximately 78 kb 3' flanking region of the *lhb* gene, was found to be best suited. A humanized renilla GFP (hrGFPII)-Km cassette containing kanamycin resistant gene and the *gfp* sequence (with start codon and kozak sequence), a stop signal and a polyA tail, was used as a template in a PCR reaction, where two primers were designed with the purpose of adding *lhb* gene-specifc arm sequences to the hrGFPII-Km cassette. A linear fragment DNA cassette containing hrGFPII with sequences homologous to *lhb* on both sides was generated by this PCR amplification. The PCR product was then incorporated into the BAC just upstream of the translation initiation site (ATG) of the *lhb* gene by homologous

recombination. The obtained construct then had the *gfp* coding sequence followed by a polyA signal that disrupted the *lhb*-coding region in the BAC (figure 12).

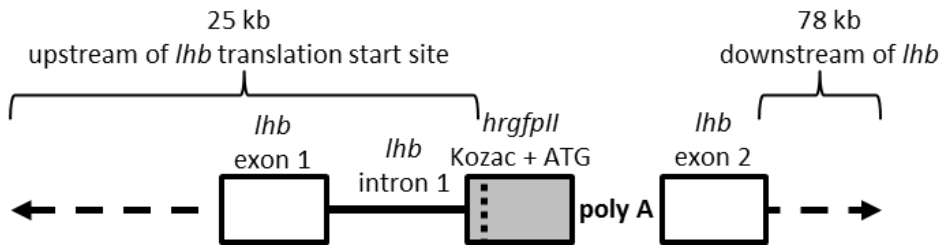

Figure 12 Schematic figure of the region in the BAC that contains the *lhb* sequence and the hrGFPII cassette.

2.4 Quantification of mRNA expression using qPCR assay

The qPCR assay for quantification of mRNA expression was performed using a LightCycler 480 Real-Time PCR system (Roche Diagnostics GmbH, Mannheim, Germany), using the LightCycler 480 Master with SYBR green I non-specific detection. SYBR Green I detection dye binds to all double stranded DNA, including the amplified PCR product. Because of this non-specific detection of DNA, the qPCR assays had to be carefully evaluated by performing a melting curve analysis. Melting curve analysis was performed immediately after the qPCR, within the same LightCycler 480 machine without breaking the seal over the samples. This removes the risk of contamination and pipetting errors. To avoid detection of potential traces of gDNA, the primers or the amplicon was designed to span exon-exon boundaries based on *in silico* analysis of the medaka genome. A standard dilution curve was run in triplicate for each primer pair to determine the primer pair with the best PCR reaction efficiency.

2.4.1 Preparations of the samples

Eggs were collected just after initiation of light in the morning and were immediately placed in E3 medium on ice until visual inspection under a dissecting microscope. After synchronization the eggs were confirmed to be 0 hpf and were put in an incubator at 28°C. For gene expression analysis, developing embryos and larva were pooled and transferred to RNA later (Ambion, TX, USA) at specific time points (table 2). The samples were stored at -20°C before RNA was extracted.

Table 2 Number of eggs from each stage used for gene expression analysis and the mean amount of RNA extracted from each stage.

Sample	Eggs per pool	Mean RNA amount (pr pool)	Mean RNA amount (pr embryo)
1 hpf	40	137 ng/µl	3.43 ng/µl
18 hpf	30	135 ng/µl	4.5 ng/µl
24 hpf	20	99 ng/µl	4.95 ng/µl
30 hpf	20	130 ng/µl	6.5 ng/µl
36 hpf	20	135 ng/µl	6.75 ng/µl
48 hpf	20	279 ng/µl	13.95 ng/µl
72 hpf	15	340 ng/µl	22.67 ng/µl
96 hpf	15	467 ng/µl	31.13 ng/µl
120 hpf	10	441 ng/µl	44.1 ng/µl
8 dpf	2	129 ng/µl	64.5 ng/µl
11 dpf	2	125 ng/µl	62.5 ng/µl
14 dpf	2	107 ng/µl	53.5 ng/µl

RNA extraction and purification were performed following the protocol for RNeasy Lipid Tissue Mini Kit (Qiagen, Hilden, Germany) with on-column DNase treatment (Qiagen). The eggs were transferred from RNA later (Ambion) to tubes containing lysing Matrix D (MP Biomedicals, Solon, OH, USA) and 1 ml Qiazol (Qiagen). A FastPrep -24 Tissue and Cell Homogenizer (MP Biomedicals, Solon, OH, USA) was used to homogenize the samples. The FastPrep instrument ran for 40 s with speed 4 m/s. The tubes were then put on ice for 2 min to avoid over-heating and degradation then homogenized once more with the same settings, before another 2 min of cooling. The homogenized tissue was incubated for 10 min at room temperature to promote the dissociation of nucleoprotein complexes. Next, 200 µl of chloroform was added, before the tubes were vigorously shaken for 15 s and the homogenate was placed at room temperature for 2-3 min. The samples were centrifuged at 12,000 g for 15 min at 4 °C. During centrifugation, the samples were separated in three phases; an upper colorless phase containing RNA, a white interphase and a pink organic phase in the bottom of the tube. The upper aqueous phase was transferred to a new tube, before addition of 1 volume of 70 % ethanol then vortexed. The sample was transferred to an RNeasy Mini spin column, centrifuged at room temperature for 1 min at 8000 g and put at room temperature for 1 min. The flow through was discarded. DNase treatment was performed by washing the membrane with Buffer RW1 followed by centrifugation and addition of 10 µl of DNase I stock solution

mixed with 70 µl Buffer RDD to the RNeasy spin column membrane and incubation at room temperature for 15 min. The membrane was washed once more with Buffer RW1 and centrifuged. The membrane of the RNeasy spin column was washed with washing buffers Buffer RW1 and Buffer RPE. To elute RNA 30 µl RNase-free water was added directly onto the membrane of the column and centrifuged. NanoDrop (Thermo Fisher scientific, USA) and Bioanalyzer 2100 (Agilent technologies, Santa Clara, USA) were used to control the amount and quality, respectively, of the RNA. RNA quality is estimated with a RNA integrity number (RIN) value that ranges from 10 (intact) to 1 (totally degraded).

SuperScript III reverse transcriptase (Invitrogen, Carlsbad, CA, USA) and Oligo(dT) (Invitrogen) were used to prepare cDNA from 1 µg total RNA according to standard protocol. Molecular grade water was mixed with 1 µl of Oligo(dT) primers (50 µM), 1 µl of dNTP mix (10 mM) and 1 µg RNA to a final volume of 13 µl and incubated at 65 °C for 5 min, followed by incubation on ice for 1 min. After incubation, 4 µl of 5X First-Strand Buffer, 1 µl 0.1 M DTT (0.1 M), 1 µl RNase OUT recombinant RNase inhibitor (40 U/µl, Invitrogen) and 1 µl SuperScript III Reverse transcriptase (200 U/µl) was added. The reaction was mixed and incubated at 50 °C for 60 min followed by inactivation at 70 °C for 15 min.

2.4.2 qPCR assay

qPCR was performed with primers for *lhb*, which was the gene of interest, and *16s* ribosomal RNA (*16s* rRNA) used as a reference gene to normalize the expression of the target gene. rRNAs, which constitute 85 – 90% of total cellular RNA, are useful internal controls, as the various rRNA transcripts are generated by a distinct polymerase (for review, see Paule and White, 2000) and their levels are less likely to vary under conditions that affect the expression of mRNAs (Barbu and Dautry, 1989). Each sample was analyzed in duplicate reactions each consisting of 5 µl SYBR Green I master mix (Roche), 2 µl of forward and reverse primer mix (5 µM each) and 3 µl of 10x diluted cDNA sample in a total volume of 10 µl. A non-template control (NTC), which contained nuclease-free water (Ambion) instead of cDNA, was included in duplicate for every primer pair on every plate. After the initial Taq activation at 95 °C for 10 min, LightCycler PCR was performed using 42 cycles consisting of 10 s at 95 °C, 5 s at 60 °C and elongation at 72 °C for 4 or 5 s (for *lhb* and *16s*, with amplicon lengths of 100 bp and 120 bp, respectively). The fluorescence was measured at the end of each cycle. A melting curve analysis was performed directly following the qPCR to evaluate whether only

one specific product had been amplified. The melting curve analysis were performed by continuously reading the fluorescence while slowly increasing the temperature from 65 °C to 95 °C. NTC controlled for non-specific contamination and melting curve analysis was run to verify that a single specific product was measured in each run. A calibrator (a mix of all the cDNA used in the experiment) was added to each plate to control for interassay variations. A sub-sample (n=5) of no-rt (reverse transcriptase) controls was run to confirm the lack of gDNA amplification.

The relationship between increasingly diluted cDNA and the corresponding Cq (quantification cycle) value was used to produce dilution curves. After running a qPCR with the dilution series, the Cq values were plotted against the logarithm of the relative cDNA concentration. The qPCR efficiency (E) was calculated using the slope of the regression line (Equation 2). A slope of -3.32 gives an efficiency of the qPCR equal to 2 (100%), which means that there is a doubling of product for each PCR cycle.

Equation 2

$$\text{Efficiency} = 10^{-1/\text{slope}}$$

The cDNA used for gene expression analysis had a 1:10 dilution. An efficiency adjusted quantification method (equation 3) (Fleige et al., 2006; Weltzien et al., 2005) was used to calculate the relative expression change of the *lhb* gene relative to the *16s* reference gene expression.

Equation 3

$$R = \frac{(E_{ref})^{Cq\,sample}}{(E_{target})^{Cq\,sample}}$$

2.4.3 Statistical analysis of qPCR data

qPCR data were first tested for homogenous variance and then analyzed by one-way analysis of variance (ANOVA), to calculate whether there was a significant difference between the expression of *lhb* mRNA transcripts in the different stages investigated during medaka embryogenesis. A Turkey-Kramer HSD post-hoc analysis were performed to determine which groups that were significantly different ($p<0.05$).

2.5 Co-localization of *lhb* and Gfp expression in medaka embryos

Our group had earlier demonstrated co-localization of Gfp and *lhb* in the pituitary of adult medaka and I wanted to determine if the same co-localization existed in embryos, thus whether the Gfp expression observed in the larvae represented the *lhb* expression of our interest. Multiple attempts of whole mount *in situ* hybridization (ISH) of *lhb* in medaka larvae were performed, but there was no transcripts detected. A co-localization experiment where Gfp positive cells were dissected out of the larvae and RT-PCR reactions with primers for *lhb* and *gfp* was therefore performed. The pituitary gene marker *lhx3* was also tested on the Gfp positive cells to investigate if the cells were located in the developing pituitary.

2.5.1 RT-PCR on dissected Gfp positive cells

To investigate this co-localization, RT-PCR reactions with primers for *gfp, lhb* and *lhx3* were performed on Gfp positive cells. To only detect endogenous *lhb*, the *lhb* primers were designed to span the *gfp* sequence, which disrupts the *lhb* gene in the BAC. When the primers are localized on each side of the *gfp* sequence, the amplicon will be too long to be amplified within the given elongation time, and the *lhb* gene from the BAC will not be amplified in the PCR reaction. Three days old transgenic embryos (n = 10) were placed in petri dishes filled with 1x PBS under a fluorescent dissecting microscope. The Gfp positive cells were dissected out using fine tweezers. The egg was first de-chorionated by punching a hole in the chorion with one tweezer and using the other to rip open the chorion, then the head and tail region of the embryo was cut off. The remaining Gfp negative tissue was removed piece by piece by holding the tissue with both tweezers and pulling them slowly apart. The Gfp positive cells were collected, and put directly in 0.2 ml PCR tubes containing 10 µl Cells Direct (Invitrogen).

The samples in Cells Direct (Invitrogen) were incubated in a thermal cycler (Mastercycler gradient, Eppendorf) at 75 °C for 10 min to lyse the cells. After incubation, DNase treatment with TURBO DNase-free kit (Ambion, TX, USA) was performed to eliminate any potential gDNA remaining in the extracted RNA. The DNase treatment was performed according to the manufacturer's protocol, adding 0.1 volume 10X TURBO DNase buffer and 1 µl TURBO DNase to the RNA. The tube was incubated at 37 °C for 20 – 30 min. After the incubation, 0.1 volume of DNase inactivation reagent was added and mixed well. The tube was incubated

at room temperature for 5 min with occasional mixing followed by centrifugation at 10,000 g for 1.5 min. The supernatant containing RNA (10 µl) was transferred to a new Eppendorf tube. The quantity of DNase treated RNA was measured using the NanoDrop spectrophotometer (NanoDrop, Thermo Fisher scientific).

For first-strand cDNA synthesis, 8 µl RNA, 1 µl dNTP and 1 µl Oligo d(T) was incubated at 65 °C for 5 min. After 1 min incubation on ice, 2 µl 10x buffer RT, 4 µl 25 mM $MgCl_2$, 2 µl 0.1 M DTT, 1 µl RNase OUT and 1 µl Superscript III was added. The reaction samples were incubated at 50 °C for 50 min, before being inactivated at 85 °C for 5 min.

Platinum Taq DNA polymerase (Invitrogen) was used to perform a PCR with primer pairs for *lhb*, *gfp* and *lhx3*, the latter being a genetic marker specific to the pituitary that was included to evaluate whether the dissected tissue included cells from the developing pituitary. The primers for the pituitary genetic marker would thus determine if there was any pituitary tissue in our samples. To control the quantity of cDNA, a PCR with primers for the reference gene *bactin* was performed on all the samples. The reactions were run on a thermal cycler (Mastercycler gradient, Eppendorf) with the same parameters as in section 2.1.1, except from the elongation step which was run at 72 °C for 1 min, 15 sec. This was followed by 10 min of elongation at 72 °C. A gradient was used because the *lhx3* primers have a melting temperature of 50 °C, and the primer pairs for *lhb*, *gfp* and *bactin* have melting temperatures of 55 °C. The PCR products were run on a 2% agarose gel, to analyze the products from the different PCR reactions.

2.5.2 Sequencing of *lhb* PCR product

The gel band representing the *lhb* PCR product was extracted from the gel, purified, and sequenced at the ABI-lab at the University of Oslo.

2.6 Imaging and qualitative analysis of Gfp expression

2.6.1 Larval handling for qualitative analysis

According to the description in section 2.2.2, eggs for imaging were collected right after fertilization and synchronized at the one cell stage. After synchronization eggs were incubated at 28 °C.

When the larvae used for confocal microscopy reached the right stage, they were transferred from medium to 1 x PBS to wash the eggs and remove the medium completely. The medium contains methyl blue, and the eggs would have a blue color after fixation if the medium was not removed. After washing, the eggs were fixed in 4 % paraformaldehyde (PFA) at 4 °C for 6 – 12 hours. When fixed, the larvae were de-chorionated (described in section 2.5.1) by using fine tweezers and a dissecting microscope. To get a good visualization of the larvae in the microscope the yolk sac should be removed. This was done by holding the yolk sac with both tweezers and then pulling the tweezers apart. This destroyed the yolk sac and it could be removed piece by piece. After dissection each larvae was placed in a droplet of 1% agarose to stabilize it in the desired angle for imaging.

2.6.2 Confocal microscopy

Confocal microscopy gives a better resolution compared to fluorescence microscopy because it uses point-illumination and a spatial pinhole. The result of this technique is that it eliminates out-of-focus light in specimens that are thicker than the focal plane (Claxton et al., 2006). Because of this, the picture comes from a thin section of the sample. By scanning many thin sections, these can be put together and made into a three-dimensional image of the sample.

An Olympus FluoView 1000 upright BX61WI confocal laser scanning microscope (Olympus, Center Valley, PA, USA) was used for this part of the qualitative analyses of larval development. Pictures were taken in planes, separated by z-axis steps varying between 0.4 and 1 µm. Picture size were set to 1024 x 1024 pixels, 4 µs/pixel. Fluorochromes were excited with a 488 nm Argon laser to detect Gfp expression.

Three-dimensional representations of the Gfp positive cells in medaka were produced using Imaris (6.3.0 v., Bitplane AG, Zürich, Switzerland), a 3D image processing and analysis software, based on picture information from the confocal microscope. The processing done with Imaris included studying the Gfp expression with and without the transmission picture or as a 3D-representation, analysis of individual optical sections and to adjust the fluorescence to get a representative image.

2.6.3 *In vivo* qualitative analysis

The embryos were synchronized to one cell stage when collected and observed in an Olympus IX81-fluorescent microscope (Olympus, Tokyo, Japan). After initial observations, we estimated that the observation of Gfp expression should be performed every 30 min from 24 hpf and onwards to see when the Gfp expression first started. The developmental expression analysis was performed on larvae from 48 hpf to 14 dpf and the larvae were studied every 12 – 24 hours. The eggs were placed in individual wells, covered by E3 medium during observation. This ensured that the embryos were stable during the expression analysis and made it easy to separate the different eggs from each other. Because the embryonic development is affected by temperature, room temperature was kept constant at 27 °C during the observations. Hatched larvae were anaesthetized with benzocaine (0.2-0.5 mg/ml) (Sigma-Aldrich, USA) before the observations.

2.7 *In situ* hybridization

ISH is a type of hybridization that uses a labeled complementary DNA or RNA strand to localize a specific DNA or RNA sequence in a portion or section of tissue. For ISH analysis of larvae, histological sections were prepared by fixation of the specimen in a mixture of 80 % HistoChoice (Sigma-Aldrich, St Louis, MO, USA), 2% PFA, 1% sucrose, 1% CaCl2 and 0.05% glutaraldehyde. Larvae were initially fixed for 5 hours, dissected out of their chorion and then fixed for an additional four hours. Hatched juvenile medaka were anesthetized on ice and placed directly in the fixation medium overnight at 4 °C. Fixed specimen were then dehydrated in serial methanol washes (70%, 80%, 95%, 100%) for 20 min x2 each and kept in 100% ethanol at -20 °C for a minimum of 18 hours. Fixed and dehydrated specimen were then cleared in chloroform 30 min x4 at room temperature and infiltrated with paraffin wax for 30 min x4. Paraffin blocks were made for the embedded medaka and kept at 4 °C until

sectioning. Three to six µm sections were prepared using a horizontal microtome (Thermo Scientific, Waltham, MA, USA), dried at 37 °C and stored at 4 °C.

Digoxigenin (DIG) labeled riboprobes were generated by *in vitro* transcription according to the manufacturer's protocol (Roche) of cloned sense and antisense sequences to detect the tissue distribution of *lhb*, *fshb*, *pit1*, and *lhx3* by whole mount and tissue section ISH. Because DIG is a protein only found in plants, the risk of cross-reactivity in the samples is eliminated. Antibodies which react with and binds to DIG express a signal (anti-DIG signal) which show where the genes are located.

For whole mount ISH, 48 hpf and 72 hpf larvae were fixed and dissected as described above using 4 % PFA. ISH was carried out according to established protocol (unpublished results, Hildahl et al 2011). Anti-DIG staining was observed using an Olympus IX81-fluorescent microscope (Olympus). Bright field imaging of the anti-DIG staining was compared with Gfp fluorescence detection.

3 Results

3.1 Generation of the tg(*fshb*:RFP) construct

The results from experiments performed throughout the process of generating the tg(*fshb*:RFP) construct are shown in section 3.1.1 to 3.1.3 below.

3.1.1 Confirmation of tg(*fshb*:RFP) construct

PCR of the *fshb* promotor

The PCR reactions with gDNA from medaka as a template and *fshb* primers gave two specific bands with the correct sizes of 4000 bp and 2500 bp, respectively (figure 13). The same reverse primer and different forward primers for *fshb* were used in the PCR reaction to get two different insert lengths of the *fshb* promotor. These PCR reactions were performed to amplify and isolate the two inserts for the tg(*fshb*:RFP) construct by gel extraction.

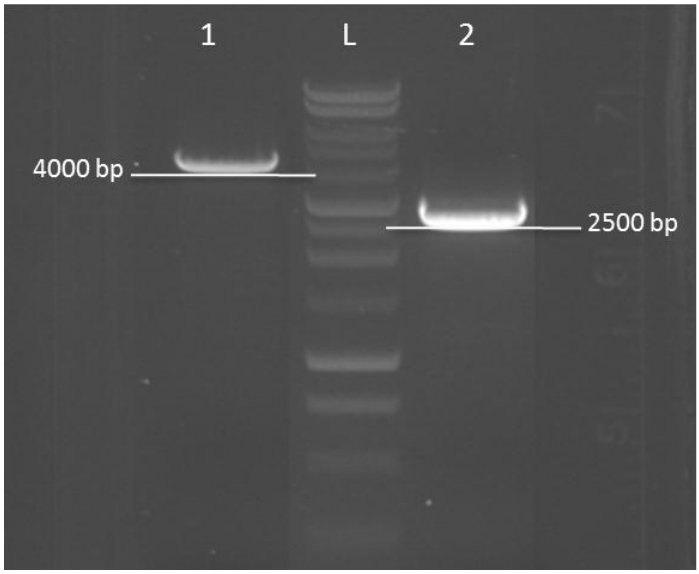

Figure 13 PCR of the *fshb* promotor. Lane 1: 4000 bp *fshb* promotor. Lane L: 1 kb ladder (Promega). Lane 2: 2500 bp *fshb* promotor.

Restriction enzyme digestion with BamHI, EcoRI and NcoI

The pGEM-T Easy vector containing the *fshb* insert and the pBluescript II SK vector with *rfp* sequence both contained restriction sites for EcoRI and BamHI. The vector and insert were required to contain the same restriction sites to generate sticky ends and thus enable the incorporation of insert into vector. In the pBluescript II SK vector with *rfp* insert, these cutting sites were located adjacent to each other and close together (figure 9) upstream of the *rfp* coding sequence. The product of this restriction enzyme digestion would thus appear as one single band on the gel. Figure 14A shows one single clear band with the expected size about 3700 bp, which was the size of the pBluescript II SK vector with *rfp* insert (3711 bp).

The cut site distribution in the pGEM-T Easy vector leads to separation of the vector and *fshb* insert following the restriction enzyme digestion. The expected band lengths were 4000 bp (*fshb*) and 3000 bp (plasmid) in the construct with the long *fshb* insert, and 2500 bp (*fshb*) and 3000 bp (plasmid) for the construct with the short *fshb* insert. The results (shown in figure 14B) correlate well with the expected band lengths.

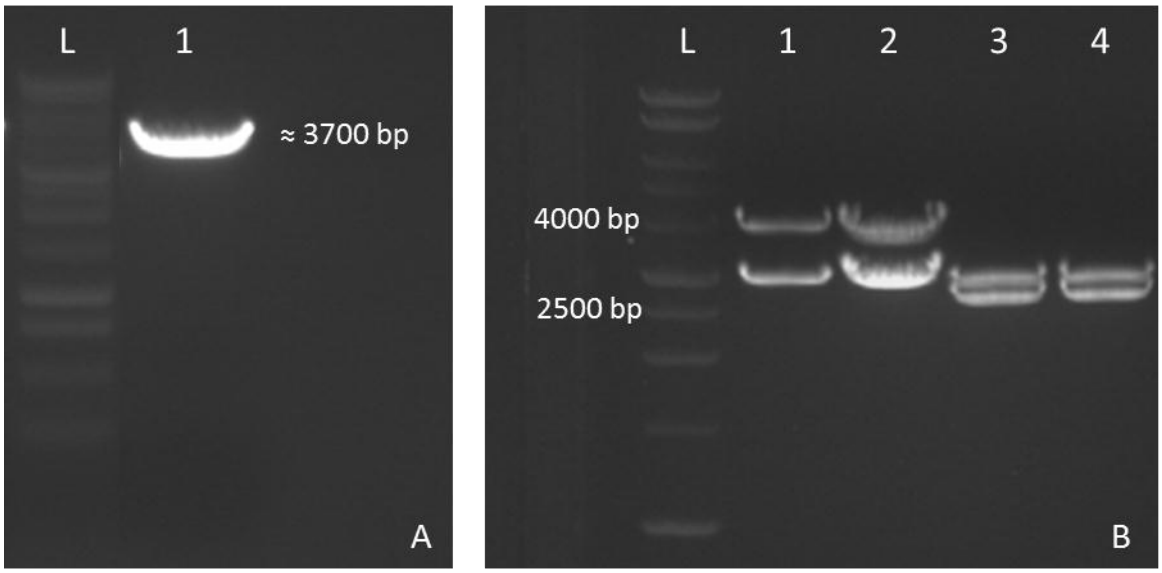

Figure 14 Restrisction enzyme digestion. A) *rfp* construct cut with BamHI and EcoRI. Line L: 1 kb ladder (Promega). Line 2: *rfp* construct cut with BamHI and EcoRI. B) Restriction enzyme digestion (BamHI, EcoRI) of two replicates of pGEM-T Easy vector containing *fshb* promotor insert. Line L: 1 kb ladder (Promega). Lines 1 and 2: 4000 bp *fshb* promotor cut out of pGEM-T Easy vector (3000 bp bands). Lines 3 and 4: 2500 bp *fshb* promotor cut out of pGEM-T Easy vector (3000 bp bands).

Following integration of the *fshb* sequence into the pBluescript II SK vector, successful ligation was confirmed by restriction enzyme digestion with NcoI. NcoI had two restriction

sites in the construct; one inside the *rfp* sequence and another inside the *fshb* sequence. The results of this digestion would confirm the presence of both *rfp* and *fshb*. The pBluescript II SK vector (3000 bp) with *rfp* insert (711 bp) resulted in a vector of 3711 bp. Depending on the *fshb* insert the complete size of the construct was either 6211 bp or 7700 bp. Both restriction enzyme digestions should give a band of approximately 2250 bp, and depending on the size of *fshb*, a second band of approximately 3960 bp or 5450 bp. As shown in figure 15, both the *rfp* and the two different *fshb* sequences were present in the vectors.

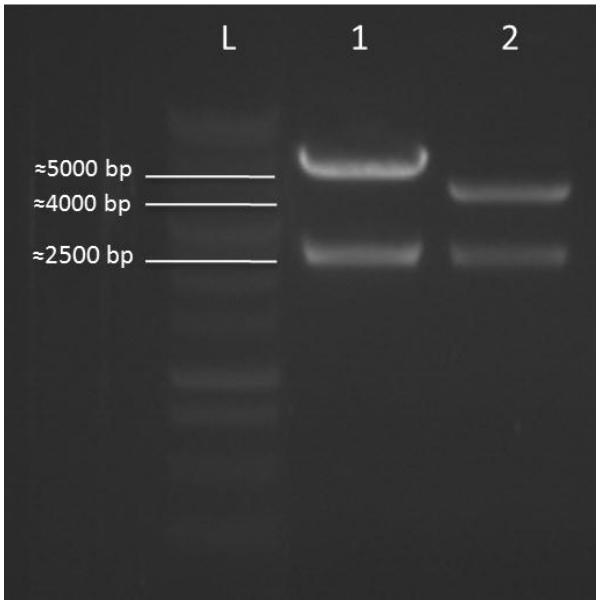

Figure 15 Restriction enzyme digestion performed with NcoI on the *rfp* vector with *fshb* insert. Line L: 1 kb ladder (Promega). Line 1: *rfp* vector with 4000 bp *fshb* insert cut with NcoI. Line 2: *rfp* vector with 2500 bp *fshb* insert cut with NcoI.

Sequencing of the tg(*fshb*:RFP) construct

Only one primer was needed for sequencing reactions. We chose to include two primers for confirmation of the *fshb* sequence and the *rfp* sequence. The pUC/M13 primer (Promega), which had a complementary sequence located immediately upstream from the start of the *fshb* sequence in the pBluescript II SK vector, was used as a forward sequencing primer. The resulting sequences showed around 900 bp of the correct *fshb* sequence for both constructs (figure 16). The *fshb* forward primer (fshbF3) annealed in the 3´end of both the short and long *fshb* sequence. Since the distance between the *fshb* and *rfp* sequences was short (the *fshb* sequence was cloned into the vector approximately 20 bp upstream of the *rfp* sequence), the sequencing results showed approximately 200 bp of the correct *fshb* sequence, the short linker region, and the whole (711 bp) *rfp* sequence.

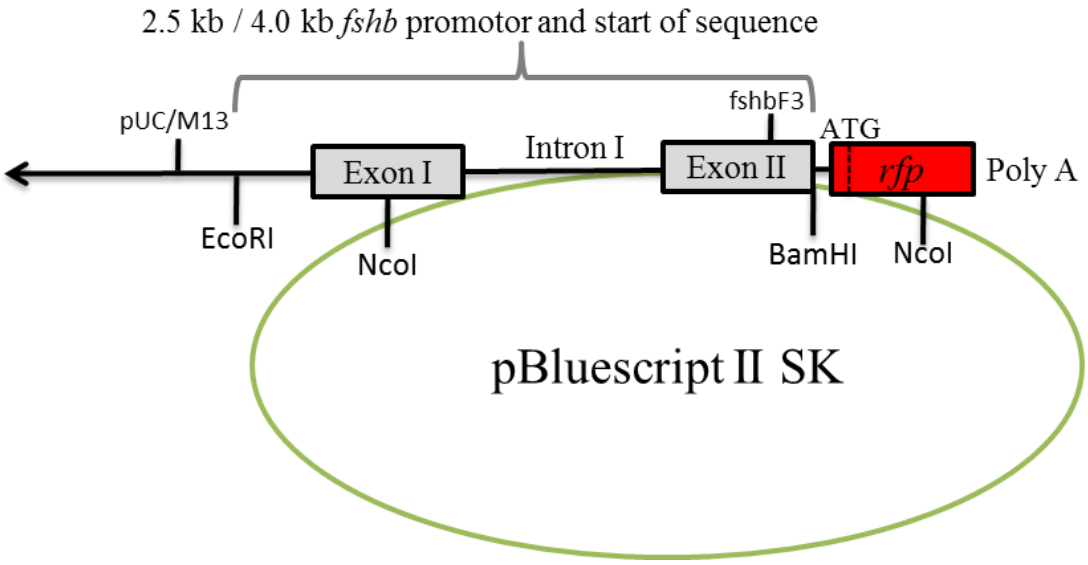

Figure 16 The tg(*fshb*:RFP) construct. 2.5 or 4.0 kb of the *fshb* promotor (3394 or 2008 bp) and the start of the sequence of *fshb* (545 bp) was inserted into the vector between the restriction sites EcoRI and BamHI. A start codon and the *rfp* sequence were localized downstream of the *fshb* promotor region. Cut sites for NcoI, that were used in the restriction enzyme digestion control of the construct, and primers used for the sequencing control are shown in the figure.

3.1.2 Microinjection and screening

When the construct had been prepared, the next step was to incorporate this transgene into the medaka genome. The construct was delivered into the cell by microinjection at one cell stage, thus enabling incorporation of the construct into the genome. Table 3 shows a survey of eggs microinjected with the two different constructs.

Table 3 Microinjection of tg(*fshb*:RFP). The table shows concentration of the construct, number of eggs injected, and death rate.

Construct	Concentration of construct	Number of injected eggs	Number of eggs that died	Positive F_0
tg(*fshb*:RFP) short (2500 bp)	2.9 ng/µl	531	135 (25%)	0
tg(*fshb*:RFP) long (4000 bp)	2.2 ng/µl	405	154 (38%)	1

About 100 eggs were injected per day. Of all eggs screened for fluorescence, one egg with Rfp expression was found. The expression was found in a restricted area in the tail region (figure 17). There are two endocrine tissues in the caudal region in fishes, the gonads and the urophysis (Evans and Claiborne, 2006). The *fshb* could be expressed in the gonads at this

stage of development, however, because we have only seen *fshb* expression in one individual, these are preliminary results and have to be investigated more closely at a later stage. The microinjected eggs that did not survive died at regular intervals, a few eggs each day until 4 dpf. The surviving larvae are at present growing to sexual maturity (expected January 2012), at which time they will be crossed with each other and the eggs will be screened for the presence of the transgene. This will not be discussed further as it is outside the scope of this master thesis.

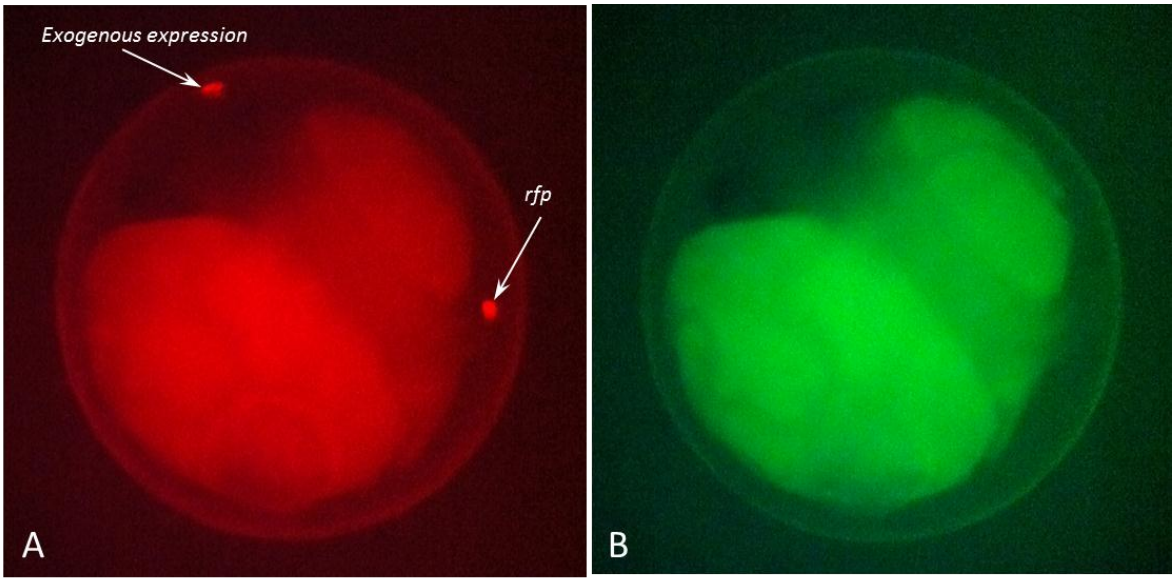

Figure 17 tg(*fshb*:RFP) positive embryo (48 hpf). A) The Rfp expression in the tail region was specific. The expression in the headregion was determined to be exogenous (outside the larva) because closer examination showed that the expression was located outside the chorion and disappeared the next day. B) The Rfp positive embryo viewed with GFP filter to confirm that the expression seen in A is not autofluorescence.

Table 4 shows a survey of eggs microinjected with constructs pre-treated with the meganuclease *I-SceI*. This restriction enzyme will cut the transgene out of the vector, and has been shown to increase the integration rate of the transgene into the host genome (Thermes et al., 2002). At the present time, no positive insertions were detected by screening.

Table 4 Microinjection of tg(*fshb*:RFP) construct pre-treated with *I-SceI*. The table shows concentration of the construct, amount of eggs injected, and death rate.

Construct	Concentration of construct	Number of injected eggs	Number of eggs that died	Positive F_0
tg(*fshb*:RFP) short (2500 bp)	2.9 ng/µl	352	163 (46%)	0
tg(*fshb*:RFP) long (4000 bp)	2.2 ng/µl	525	272 (51 %)	0

The death rate was higher in the experiment where *I-SceI* was microinjected together with the construct.

3.2 Quantitative analysis of *lhb* expression in embryonic medaka

qPCR was used to quantify the *lhb* mRNA expression in embryonic medaka. Eggs were collected in pooled samples at different developmental stages, the RNA was isolated and DNase treated, and cDNA synthesis performed. qPCR assays for *lhb* gene and *16s* reference gene were developed and validated by first performing melting curve analysis and checking the specificity of the primer pairs chosen. Melting curves that showed one specific peak indicated that the PCR only had amplified one product. The efficiency of the SYBR green I assay was evaluated using cDNA template dilution curves. The efficiency was calculated as described in section 2.3.2. The chosen primer pairs had efficiencies of 2.07 and 2.05 for *lhb* and *16s*, respectively. The Cq values ranged from 23-27 and 15-19 for *lhb* and *16s*, respectively.

lhb was clearly detected in all stages investigated. The *lhb* gene was maternally expressed during early embryogenesis, with increased transcription levels observed following initiation of zygotic expression at mid-blastula stage (18 hpf, see figure 18). Transcript levels increased up to the four-somite stage (36 hpf) followed by a decrease, reaching significantly lower levels by 120 hpf and remaining low in hatched larvae.

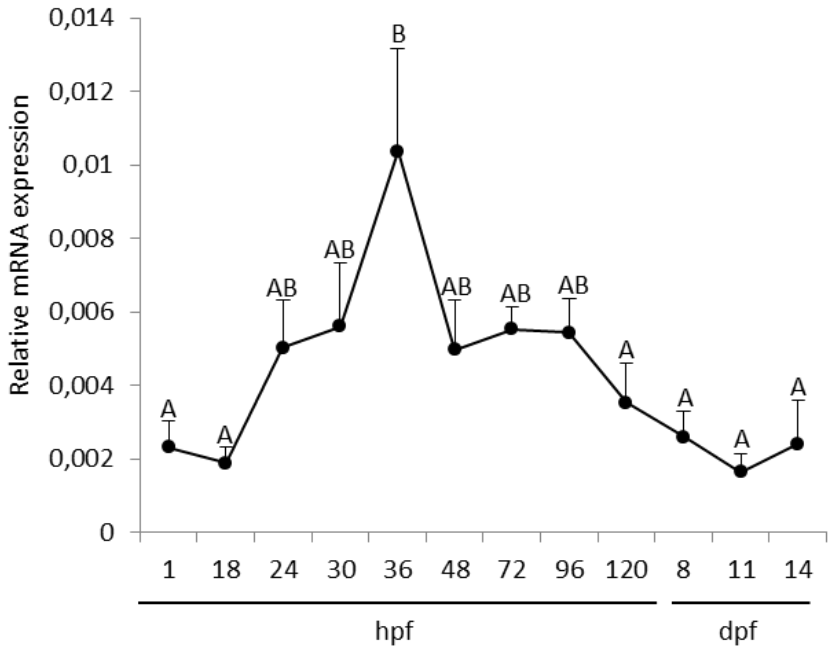

Figure 18 Quantitative analysis of lhb mRNA expression. Relative *lhb* gene expression in pooled medaka through embryonic development to post-hatch larvae. *lhb* gene expression was normalized to *16s* gene expression using an efficiency adjusted relative quantification method. Data are represented as mean relative expression + standard error of the mean (SEM), n = 4. Data were analyzed by 1-way ANOVA and differences were considered significant at $p<0.05$. The number of individuals per pool is given in table 2.

3.3 Co-localization of *lhb* and *gfp*

Since ISH proved ineffective to determine the co-localization of Gfp and *lhb* (no *lhb* was detected by this technique in larvae), RT-PCR reactions with primers for *bactin*, *lhb*, *gfp* and *lhx3* were performed using cDNA from micro-dissected Gfp-positive cells as template to confirm that Gfp and *lhb* was expressed in the same cells, and whether these cells were found in tissue outside the pituitary. To only amplify the endogenous *lhb* in the PCR reaction, the primers or the amplicon were designed to span exon-exon boundaries. As a control to confirm the absence of developing pituitary tissue contamination in the dissected samples, analysis of a pituitary marker gene, *lhx3*, was performed. The expected size of the PCR products for *bactin*, *gfp* and *lhb* was 89 bp, 233 bp and 319 bp, respectively. These sizes correlate well with the bands on the gel shown in figure 19. The PCR reaction for *lhx3* gave no specific product (expected size, 1176 bp). From these results one can conclude that *gfp* and *lhb* were expressed in the same cells, and that these cells are not located in the pituitary.

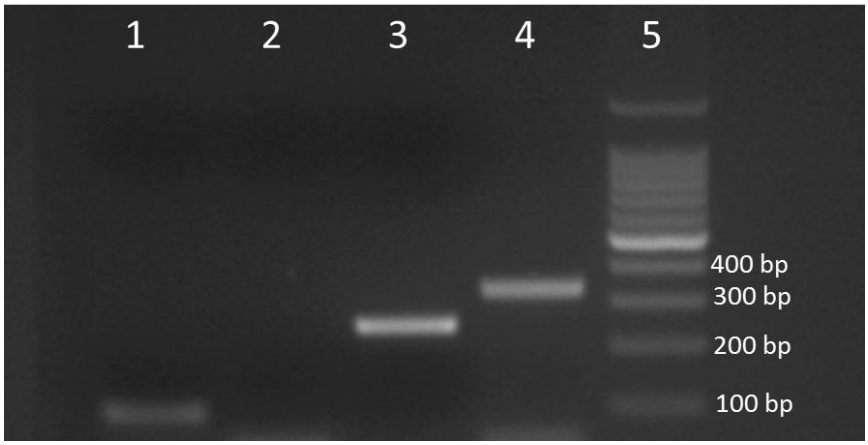

Figure 19 Co-localization gel. The PCR products visualized on a 2 % agarose gel. Lane 1: PCR sample with specific primers for the reference gene *bactin* containing a 89 bp product. Lane 2: PCR sample with specific primers for *lhx3* (1171 bp product), a gene marker specific to the pituitary. Lane 3: PCR sample with specific primers for *gfp* containing a 233 bp product. Lane 4: PCR sample with specific primers for *lhb* containing a 319 bp product. Lane 5: 1 kb ladder (Promega).

3.4 Imaging and qualitative analysis of tg(*lhb*:GFP) expression

Observation and analysis of the larvae started from 24 hpf and continued until hatching (7-9 dpf). The hatched larvae were examined around 12-14 dpf (about one week after hatching). The embryos were mostly examined in a fluorescent microscope but some selected developmental stages were studied in detail in a confocal microscope.

At least 10 individuals were examined for each stage investigated. Initially, the embryos were investigated every day (from 1-7 dpf), followed by a closer examination of the stages where most variation in the Gfp expression was found.

3.4.1 *In vivo* qualitative analysis – first expression

Special interest was directed to when and where the Gfp-*lhb* expression first occurred. The expression was closely followed the first seven hours after initial detection, at which time the expression underwent a rapid change (figure 20).

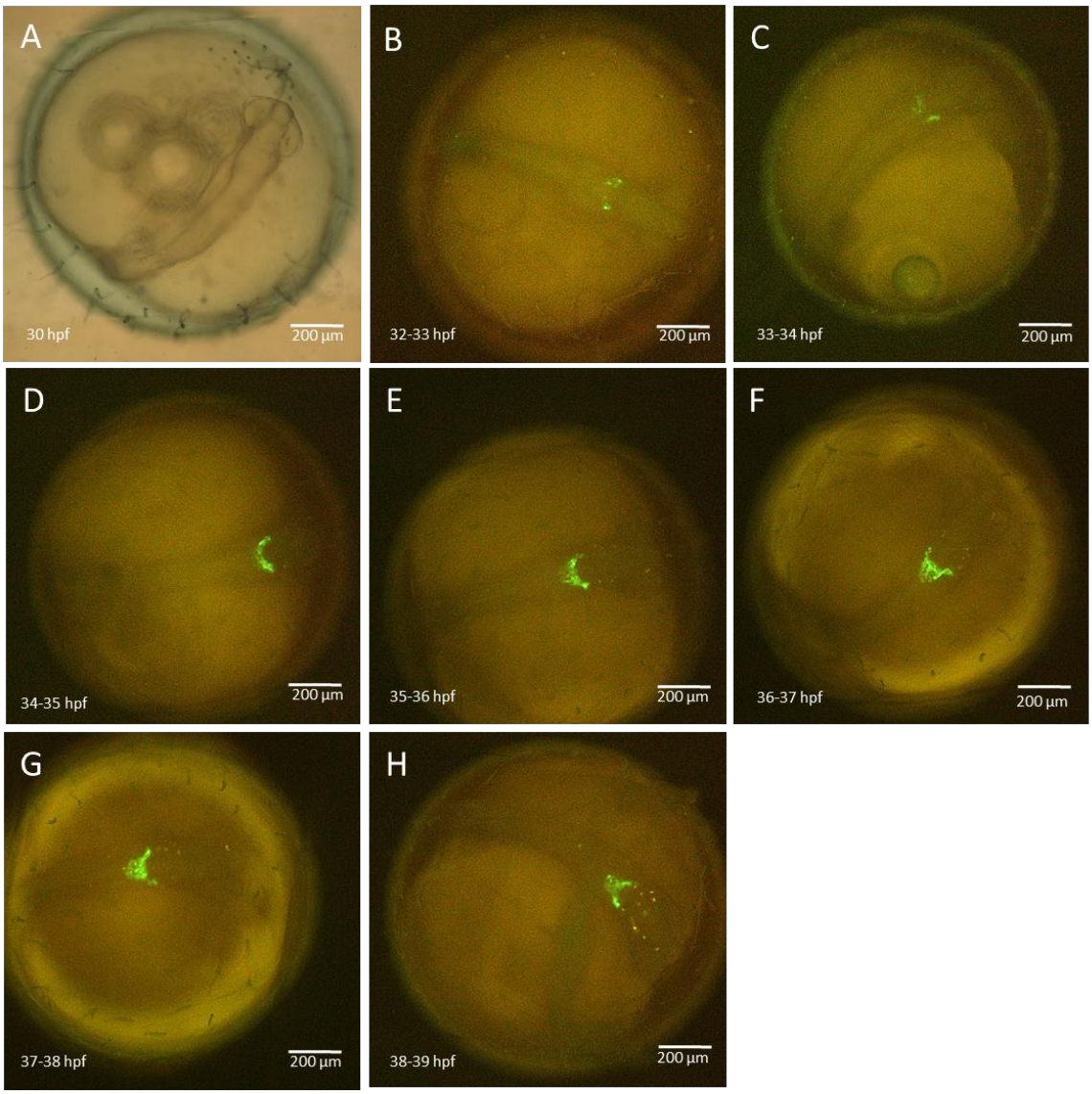

Figure 20 First expression of *lhb* in medaka embryos. A) Light image of a medaka embryo at 30 hpf. B-H) Fluorescent images of medaka embryos. Gfp expression was first observed after 32 – 33 hpf as paired lateral clusters located at the anterior margin of the otic vesicles (B). After 2 hours the expression extended to the midline (E) and more caudally (35-39 hpf, E-H).

There was no specific Gfp expression before 30 hpf. As seen in figure 20B, the first Gfp protein expression was detected in the four-somite stage (32-33 hpf, approximately developmental stage 20). Gfp expression started as paired lateral clusters posterior of the eyes and at the anterior margin of the otic vesicles. After only a few hours, the Gfp positive cells increased in number, extending to the midline (figure 20D) and posteriorly (figure 20E-H) as a continuous group of cells. By the nine-somite stage (stage 22, 38 hpf) the cells started to approach the area where the expression would dominate from 48-120 hpf (figure 21).

3.4.2 Developmental expression

When observing Gfp-lhb during embryonic development each day from 48 hpf until hatching, we found that there was few changes in the main expression pattern during this period, however, there was some alterations in the more dispersed Gfp positive cells.

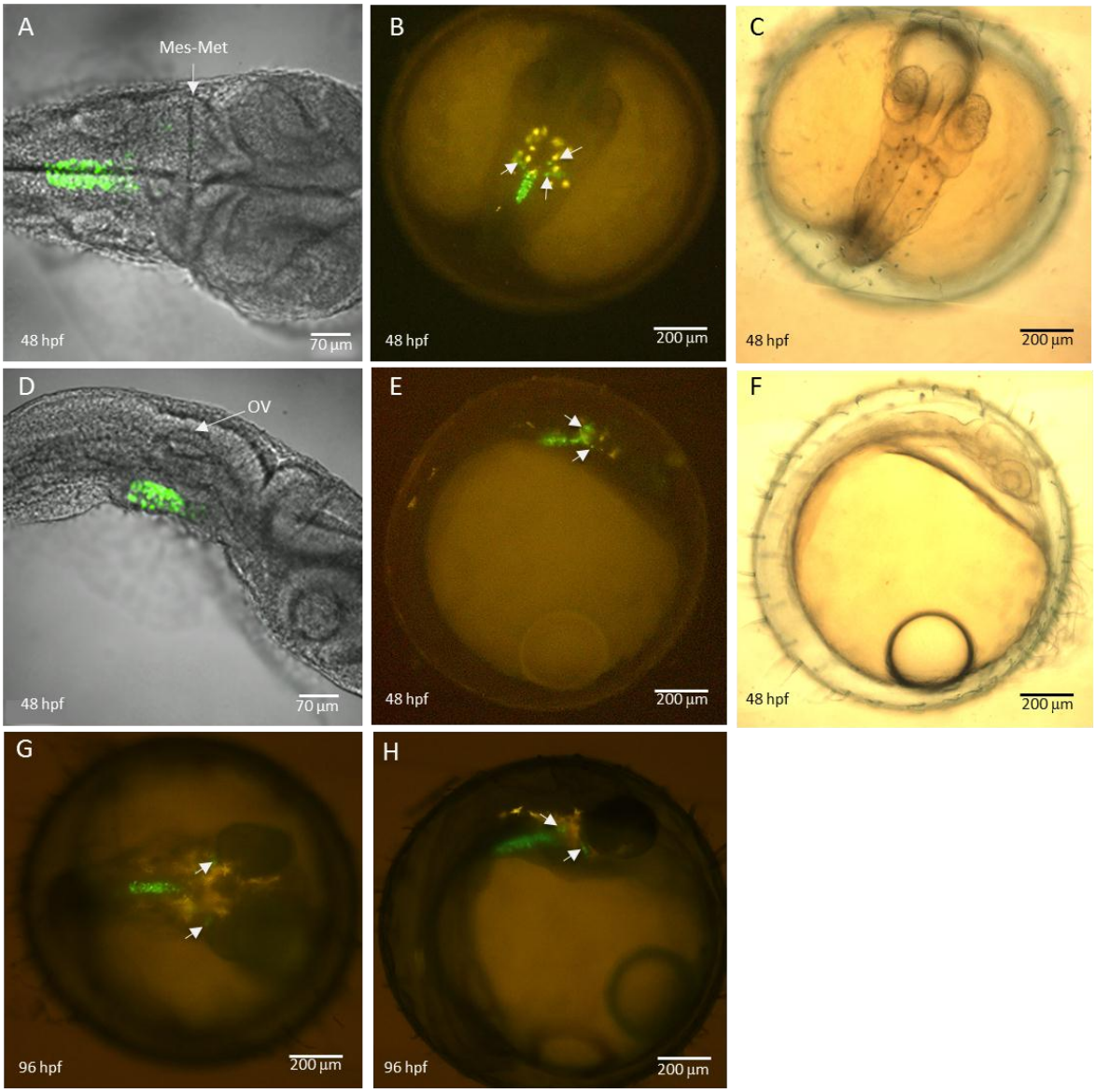

Figure 21 Gfp expression in the tg(*lhb*:GFP) medaka embryo at different developmental stages. A-F) Larvae at 48 hpf, pictures taken with confocal microscope (A, D) fluorescent microscope (B, E) and light microscope (C, F). The Gfp expression is at 48 hpf centered at the midline between the otic vesicles (OV) with a few dispersed cells located anterior of the otic vesicles. These cells are marked with arrows in B and E. All expression ended before the mesencephalon-metencephalon (Mes-Met) border. The basic Gfp expression pattern is largely established by 48 hpf, with Gfp distribution expanding only slightly as development progresses. Light microscopic images (C, F) show the orientation and anatomy of 48 hpf larvae. Larvae are orientated with the head to the right.

Figure 21A-F shows pictures of larvae at 48 hpf (the 16-somite stage). At this time the Gfp expression was centered at the midline (as seen in figure 21A ventral view, and B dorsal view) and positioned ventral in the larvae (as seen in figure 21D and E, lateral view). The Gfp expression started posterior of the developing otoliths (OV; otic vesicle, marked in figure 21D) and extended the whole length of these structures. Anterior of the otic vesicle, the Gfp expression are more dispersed and only a few cells were visible. The most anterior expression was difficult to see because of auto-fluorescence (yellow color) produced by pigment cells covering this area. The Gfp expression stopped before the mesencephalon-metencephalon (mes-met) border of the developing hindbrain (shown in figure 21A). The Gfp expression expanded only slightly relative to the growth of the larvae. By 96 hpf, there were fewer dispersed Gfp producing cells which extended to the mes-met boundary and a few distinct cells were located at the posterior margin of the eye (figure 21G-H, marked with arrows).

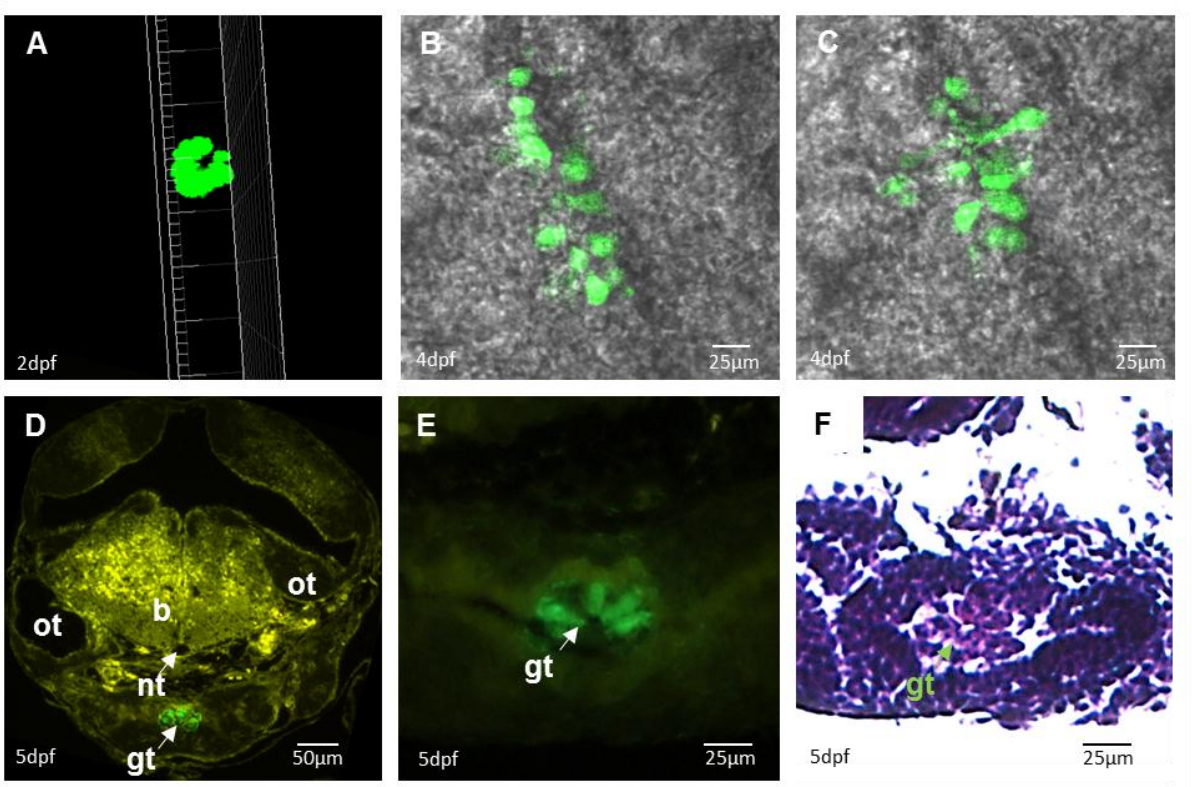

Figure 22 Embryonic tissue-specific distribution. Tissue specific Gfp expression was analyzed by confocal microscopy (B-C)) and fluorescent microscopy (D-E) and hematoxylin/eosin staining (F) of histological sections. Three dimensional rendering of confocal image analysis shows these cells are arranged in a tubular-like structure (A). Optical sections obtained by confocal microscopy display changing cell morphology in distal (B) and medial (C) planes. In transverse sections of 5 dpf larvae, Gfp is expressed in the gut tube in the ventral margin of the fish (D). Arrows identify Gfp expressing cells. Tissues are labeled as brain (b), gut tube (gt), notochord (nt) and otic vesicle (ot).

The picture-editing program Imaris was used to process the images of Gfp expressing cells into a 3D model (figure 22A). Figure 22A shows a tubular structure of the Gfp expression when the 3D model was rotated and observed as in a transverse section. Confocal images were taken as optical sections, a z-stack, through a section of tissue, such that individual planes of the image can be analyzed separately. When studying the different layers of the larvae, the Gfp positive cells were sectioned at different angles because of their tubular orientation. The section of Gfp positive cells in the dorsal and ventral part of the larvae showed a round shape (figure 22B) as the cells were sectioned in a dorso-ventral orientation. When the Gfp positive cells were sectioned in a distal-medial orientation, medially in the larvae, the shape was elongated and columnar (figure 22C). These data indicate that the Gfp positive cells have a columnar shape and are organized in a tubular arrangement. The anatomical organization of Gfp positive cells was supported by fluorescent and histological imaging of sections. Gfp positive cells were detected as a tubular structure in the ventral abdomen of 5 dpf larvae (figure 22D-E), which was identified as the developing gut by histological hematoxylin/eosin staining. This staining technique simplifies the process of recognizing different tissues or organelles in a specimen. Hematoxylin stains the nuclei of the cells blue and eosin is used as a counterstain, staining all eosinophilic structures in various shades of red, pink and orange (figure 22F). Gfp was expressed throughout the radial axis of the developing gut tube, which formed a singular radial layer of cells. By 5 dpf the lumen of the gut tube was clearly seen (figure 22F). After hatching the intestinal epithelium thickened and became more convoluted (figure 23D-F). Some residual yolk was present for 3-4 days after hatching (figure 23 F-G). Gfp expression was more limited post-hatch and were positioned anterior of the remaining yolk sac (figure 23A-B). The Gfp expression was detected as isolated cells in the intestinal wall up to 11 dpf (figure 23E) when the yolk was almost completely absorbed. Individual cells were also identified just posterior to the eye (figure 23B), however, these cells were determined to be localized to the dorsal and posterior surface of the first gill arch by histological sections (figure 23H-I).

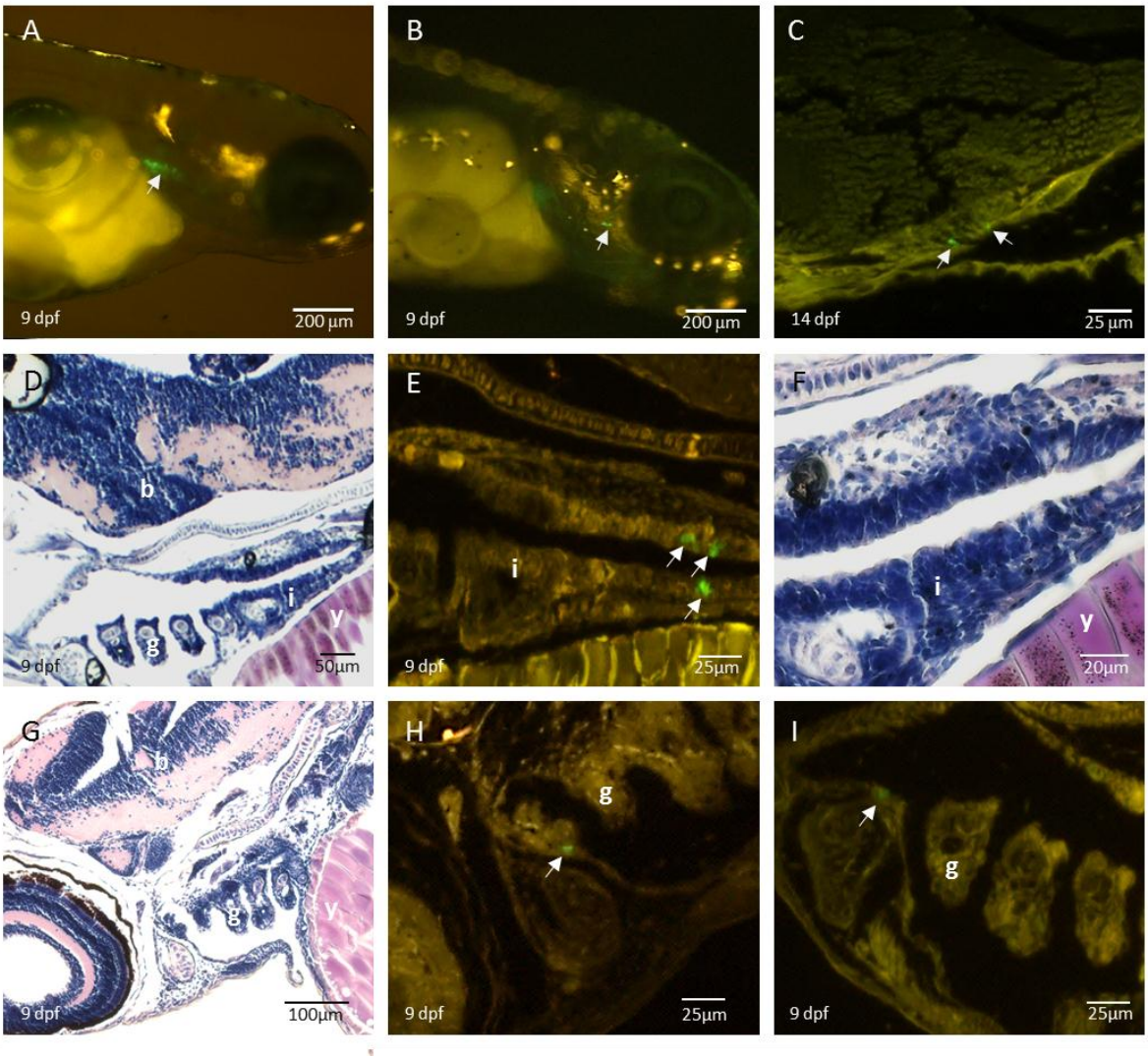

Figure 23 Gfp-*lhb* expression post hatching. When the larvae are post-hatch, the Gfp expression is greatly reduced relative to the whole larvae with isolated clusters at the dorso-anterior margin of the yolk-sac (A) and posterior margin of the eyes (B). Saggital histological sections show that Gfp is first detected in the pituitary after 14 dpf (C) and is expressed in the intestine at hatch (E). Hematoxylin/eosin staining shows anatomical structures of histological sections (D, F-G). The brain, gill arches and intestine are shown in figure D, the intestine and part of the yolk in figure F and figure G shows the brain, gill arches and the eye. Arrows identify individual cells or isolated cell clusters near the eyes (H-I), in the gut (E) and in the pituitary (C). Tissues are labeled as brain (b), gill (g), intestine (i) and yolk (y).

Pituitary Gfp expression was first detected at 14 dpf in a few isolated cells (figure 23C). The yolk was fully absorbed at this time, with no Gfp detected in the gut or in other extra-pituitary tissue.

3.5 *In situ* hybridization

Cells of the developing pituitary were localized by performing ISH using riboprobes specific for the pituitary marker genes *pit1* and *lhx3*. This experiment would determine if the Gfp-*lhb* producing cells were localized in the pituitary. ISH of pituitary marker genes showed that Lh producing cells were initially localized outside the primordial pituitary. Both *pit1* and *lhx3* were expressed in the midline ventral to the eye at 48 hpf and 72 hpf (figure 24 A and C). However, Gfp was detected posterior to the anti-DIG signal (fig 24 B and D). The otic vesicles were located at the ventral margin of the brain (figure 24 E), and Gfp was detected ventral to the otic vesicles on the basal surface of the larvae (figure 24 F). During embryonic development, thus, Gfp was primarily detected outside the central nervous system and pituitary.

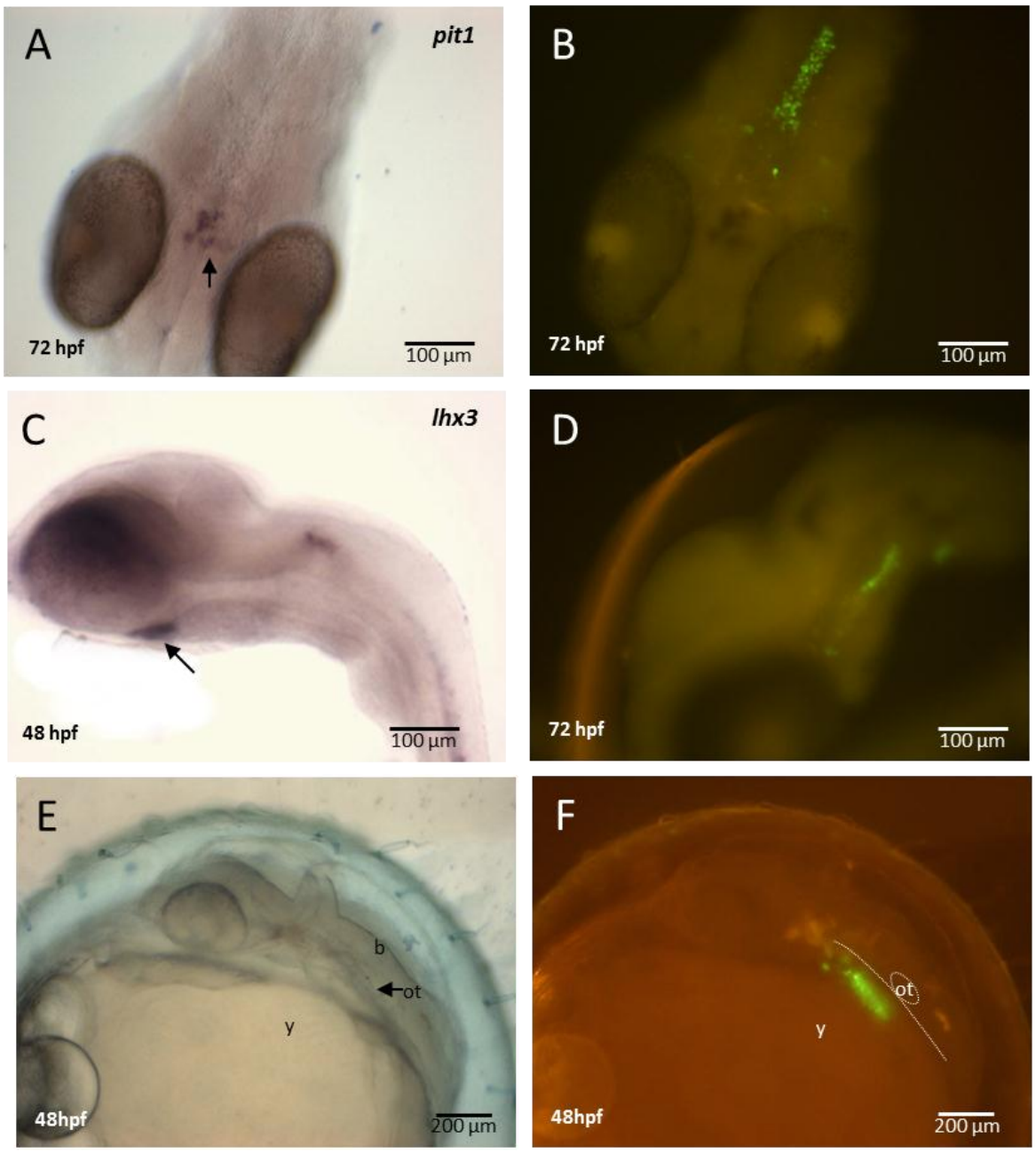

Figure 24 *lhb* expression outside the CNS. ISH with two pituitary marker genes, *pit1* (A), and *lhx3* (C), show the developing pituitary at the midline of the head and ventral to the eye (main expression identified with errors). Gfp expression starts around the anterior margin of the otic vesicle along the dorsal surface of the larva (B, D, F). The base of the larval brain is at the midpoint of the otic vesicle (E), and Gfp is clearly detected ventral to this boundary (F). Gfp is not detected in the pituitary before 14 dpf. Larvae are situated with the head to the left. Identified tissues are b, brain; ot, otic vesicle (identified by arrow and hatched line) and y, yolk.

4 Discussion of results

When designing this project, the main aim was to find out when *lhb* started to be expressed in the pituitary. During the observations it was clear that *lhb* first appeared in the gut instead of the pituitary as first expected. The data concerning *lhb* expression presented in this thesis suggests a novel function of Lh during embryogenesis in medaka.

The co-localization experiments on medaka embryos confirmed the transgene specificity of the tg(*lhb*:GFP) line during development. The co-localization of Gfp and *lhb* in adult medaka had been confirmed earlier (Hildahl et al., Submitted). Thus, a sensitive method has been established for tracing the development of Lhb producing cells using *in vivo* and *in situ* fluorescent imaging of Gfp. By this means, a novel expression of the *lhb* gene during early larval development has been revealed, suggesting a developmental function for Lh independently of the BPG axis.

A transgenic construct where Rfp expression is under the control of the *fshb* promotor was also generated. This is currently being used to establish a transgenic line where the expression and functions of the second pituitary gonadotropic hormone gene, *fshb*, can be further investigated.

4.1 *lhb* expression in medaka embryos

4.1.1 *lhb* expression outside the pituitary during early development

Few studies have looked at the expression of *lhb* outside the pituitary and to my knowledge this is the first study investigating this expression during early development. In medaka, the pituitary is located at the ventral margin of the eyes at 48 hpf as indicated by *lhx3* and *pit1* expression (figure 24 A and C), similar to zebrafish (figure 5) (Nica et al., 2006; Pogoda et al., 2006). However, the experiments presented here show that Gfp is clearly not co-localized with the pituitary marker genes, and Lh does not appear to be present in the pituitary of medaka until after hatching. Rather, Lh is expressed in the developing gut tube, a tissue of endoderm origin and this suggests a novel function for Lh during development. In medaka, the gut tube formation starts at 38 hpf (stage 22) in the rostral portion (excluding the esophagous and the pharynx) of the gut and extends caudally, reaching the cloaca by 54 hpf (stage 26) (Kobayashi et al., 2006). In my experiments, Gfp was detected prior to 38 hpf

(stage 22), as two lateral clusters of cells that migrated towards the midline and then posteriorly in the larvae. Interestingly, Koyabashi (2006) reports that gut tube formation also start in the rostral part of the gut tube by migration of the rostral endodermal cells to the midline, before further development starts more caudally in the intestine. The quantitative characterization of *lhb* mRNA expression reveals that *lhb* mRNA reached maximum levels during gut tube formation, and this supports the notion that Lh is important for the development of the gut tube. When the gut tube structure is fully established, Gfp is clearly expressed in the rostral portion as a cylindrical tube like structure. The significant decrease in *lhb* expression seen in the quantitative analysis at 120 hpf supports the notion that Lh is important for the development of the gut tube. The limited expression of Gfp in the caudal portion of the gut may reflect that this region of the gut gives rise to other structures such as liver buds and swim bladder (Kobayashi et al., 2006).

The molecular structures of *fshb* and *lhb* are well conserved from teleosts to mammals, however, some studies report differences in their regulatory mechanisms of gene expression (Kanda et al., 2011). Little data is available to assess the novel expression and putative function of Lh in the gut during development. A hypothesis was presented that a lack of conserved synteny among vertebrates nearby the *lhb* gene could explain that teleosts have two different cell types secreting Lh and Fsh, while tetrapods have only one cell secreting both gonadotropins (Kanda et al., 2011). Further, the teleost *lhb* locus has no shared synteny to either tetrapod *lhb* or teleost *fshb*. This fact suggests that drastic changes occurred in the genomic environment of the *lhb* gene early in teleost evolution (Kanda et al., 2011). Moreover, this lack of conserved synteny could possibly explain the divergent extra-pituitary developmental expression of *lhb* in the gut of medaka.

4.1.2 Possible functions of *lhb* in the gut tube

The recently discovered and evolutionary related glycoproteins, Gpa2 and Gpb5, have been identified in both vertebrates and invertebrates (Dos Santos et al., 2009). The presence of these proteins in invertebrates suggests that they could be an ancestral form of the pituitary glycoprotein hormones, Fsh, Lh and Tsh. The endogenous physiological function of Gpa2 and Gpb5 remains to be elucidated, however, these hormones are suggested to have various functions in the gut in *D. melanogaster* (Sellami et al., 2011) and *C. elegans* (Oishi et al., 2009). It is interesting to note that these glycoprotein hormones, evolutionary related to Lh, are suggested to function in the gut of other organisms since this is the same tissue *lhb*

expression was found in medaka embryos. Moreover, the gonadotropic hormone receptors (*fshr* and *lhr*) are not as specific in fish as they are in humans (Braun et al., 1991; Tilly et al., 1992). In several teleost species, Fsh only bind to the Fshr, however, Lh can bind to both the Fshr and Lhr (Miwa et al., 1994; So et al., 2005; Yan et al., 1992). It has therefore been suggested that Lh has taken over some of the functions that were performed by Fsh in fish (Evans and Claiborne, 2006). Hence, one may speculate that ancestral glycoproteins have had a function in the gut, and that Lh could bind to the Gpb receptor, which could be present in the gut, similar to how it promiscuously binds to the Fsh receptor. However, functional studies are needed to test this hypothesis.

During this project it became clear that the Gfp-*lhb* expression was widespread in the gut area during early developmental phases, however, the expression ceased soon after hatching, coinciding with complete absorption of the yolk. This suggests that Lh could be important for survival in the chorionated micro-environment. The main function of Lh in the BPG axis is to control steroidogenesis. Thus, one of the possible functions that could be assigned to Lh in the gut during development is steroidogenesis. Conversion of cholesterol to pregnenolone has been shown to be critical for embryogenesis in zebrafish, since pregnenolone preserves microtubule abundance and promotes embryonic cell movement (Hsu et al., 2006). The enzyme responsible for conversion of cholesterol to pregnenolone, *cyp11a1* a member of the P450-cytochrome family (*P450scc*), is expressed in the yolk syncytial layer (ysl) of zebrafish, thus identifying an important steroidogenic tissue during development (Hsu et al., 2006). Lh drives steroidogenesis in the gonad by stimulating the uptake of cholesterol into theca (female) or leydig (male) cells and into the mitochondrion by stimulating lipoprotein receptors and steroidogenic acute regulatory protein (StAR), respectively. Subsequently, Lh stimulates the production of androgens in these cells by also stimulating gene expression of *cyp17* (*P450c17-I*), another member of the P450-cytochrome family (Zhou et al., 2007). The gut tube during early development is located immediately adjacent to the ysl (Koyabashi et al., 2006), which is responsible for initial yolk absorption. Indeed, synthesis of pregnenolone in the intestine of the green frog (*Rana esculenta*) was stimulated following incubation with cholesterol (Belvedere et al., 2001) and Lh receptors are present in the intestine of human fetuses (Abdallah et al., 2004), suggesting that the intestine could be sensitive to LH during development and act as a steroidogenic tissue. Lh could, thus, stimulate steroidogenesis in the larval gut by stimulating cholesterol uptake and *cyp17* expression, which is an important enzyme in the steroidogenic pathway. Indeed other members of my group have found that

cyp17 gene expression has an increasing trend at 36 hpf (unpublished data) when *lhb* gene expression is significantly upregulated in the developing medaka.

A few dispersed Gfp positive cells were found posterior of the eyes between 3 and 4 dpf and were still observed at 9 dpf. Histological sections showed these cells to be closely associated with the developing gill arches, with Gfp positive cells being located at dorsal and posterior surfaces of the first gill arch. Osmoregulation is another primary function of the gut during fish larval development. For example, Na/K-ATPase activity was localized to the anterior gut in the time around hatching (48-72 hpf) in zebrafish (Wallace et al., 2005). The gills can first be identified in medaka at 82 hpf (stage 31) at which point the dispersed anterior Gfp positive cells have reached the posterior margin of the eyes. The close association of the digestive tract and the gill arches suggests that the Gfp expressing cells are part of the pharyngeal tissue as no Gfp is detected in the operculum cavity. The presence of *lhb* in the anterior gut tube and in close association with the gill arches suggests that Lhb could be involved in larval osmoregulation.

Whether Lh is involved in steroidogenesis, osmoregulation, general development of the gut tube or have another function during development, is unknown. Future studies, for example knock down experiments of Lh and the Lh receptor, will give more answers to what kind of functional role Lh plays during development.

4.1.3 First detection of *lhb* in the pituitary

During qualitative analysis of the Gfp expression, by *in vivo* observation, co-localization experiments and ISH experiments, it became clear that *lhb* is not expressed in the pituitary of medaka until approximately 14 dpf. At this stage of development the yolk is completely absorbed and the larvae have started exogenous feeding. *gnrh1* and *gnrh3* are expressed by 2 dpf in medaka, and developmental tracing in transgenic medaka reveals that Gnrh neurons extend ventrally into the pituitary from between 10 – 20 dpf (Okubo et al., 2006). This is around the time that Gfp-*lhb* is first detected in the pituitary. These data suggests that *lhb* is expressed relatively late in pituitary development, when the gross morphology of the brain has been established and the hypothalamic neurons innervate the pituitary. Thus, Lh gonadotropes could require hypothalamic inputs for final gonadotrope activation, similar to the situation in sheep (Brooks et al., 1992; Szarek et al., 2008) and in rat (Aubert et al., 1985) gonadotrope maturation. This is further supported by the observation that gonadotropin

expression starts later than other anterior pituitary hormones in multiple fish and mammalian species (Asa et al., 1988; Japon et al., 1994; Laiz-Carrion et al., 2003; Saga et al., 1993; Saga et al., 1999). However, zebrafish, the fish species with the best-characterized anterior pituitary development, provides partially conflicting results. In transiently transfected zebrafish, the *lhb* promotor drives Gfp expression in the area of the pituitary by 48 hpf (Chen and Chiou, 2010), although this signal was not confirmed by co-localization with the endogenous *lhb* gene or generation of a transgenic line. Similarly, downregulation of *lhb* in mutant zebrafish suggests that *lhb* is being produced by gonadotropes by 72 hpf although cell specific expression could not be confirmed by ISH (Nica et al., 2006). This is likely due to the lower sensitivity of ISH relative to PCR. Likewise, in our experiments, *lhb* was detected by qPCR in whole larvae but could not be detected by ISH. The zebrafish pituitary gonadotropes are determined to differentiate early in development by 32 hpf (Pogoda and Hammerschmidt, 2009). However, Podoga and Hammerschmidt (2009) characterize first detection of gonadotropes in the pituitary as the presence of the common α subunit (*gpa*) and the absence of tsh β-subunit (*tshb*). Therefore, it is unknown at what point these primordial gonadotropes mature and express *lhb* and *fshb*. For example, in mammals *gpa* expression precedes *lhb* and *fshb* expression in gonadotropes. In mouse (Japon et al., 1994) *gpa* is expressed 2 days before *lhb* and 3 days before *fshb*. *gpa* is also seen prior to *lhb* and *fshb* in human gonadotropes (Pope et al., 2006). This may explain the inability to detect *lhb* transcripts in the pituitary of zebrafish when *gpa* could be detected.

The BPG axis gain full activity when the organism reaches puberty. However, the completion of the structure and components of the BPG axis mature earlier. In mammals, The BPG axis matures in the middle of the prenatal stage (Huhtaniemi, I, 1995). The BPG axis is in this stage important for brain and gonad development. Whether the situation is similar in teleosts is unknown, however, this could suggest an important role for Lh in the pituitary at an early stage.

5 Discussion of methods

Some of the methods used in this study were established and optimized for this thesis and will therefore be discussed in this section.

5.1 Generation of tg(*fshb*:RFP) line of medaka

A tg(*fshb*:GFP) construct was successfully generated using the BAC method, but there were no positive fish in the F_0 or the F_1 generation after microinjection of the construct and screening 500 fish.

Because the BAC method proved unsuccessful, a plasmid-based tg(*fshb*:RFP) construct with meganuclease sites was generated to see if we could increase the efficiency of transgene incorporation. After microinjection of ~1000 embryos with the tg(*fshb*:RFP) construct one fish was Rfp positive in the F_0 generation. The tg(*lhb*:GFP) medaka line already established in our group is the result of microinjecting 1000 embryos. The incorporation rate for that experiment was similar to our results with two positive founder fish in the F_1 generation. The microinjected fish in the tg(*fshb*:RFP) F_0 generation are now growing and will be crossed with each other when sexually mature to identify F_1 founders of tg(*fshb*:RFP). Hence, there is good probability of more positive fish in the F_1 generation.

If provided more time, several steps in the generation of the tg(*fshb*:RFP) medaka line could have been optimized. The concentration that gave the best result for the tg(*lhb*:GFP) line was 1 ng/µl. For the tg(*fshb*:RFP) line, the concentration was between 2 – 3 ng/µl because a high concentration is favorable for integration into the genome as long as the death rate do not exceed 50%. In future experiments, a titration curve of the concentration of construct should be made, to assess the optimal injection concentration. Information about amount of deformed larvae and if the larvae have a normal developmental timeline should be recorded and evaluated. During this project it became clear that after microinjection the larvae in the same batch had different developmental rates. A reason for this could be that the injected volume of construct varied, and that a larger volume could have an adverse effect on embryonic development. To avoid this problem, future studies should optimize the injection volume. The injection volume was estimated by comparing it with the oil droplets in the yolk. There are more precise methods to measure the injection volume, for example by using a drop of oil on a stage micrometer to measure the diameter of the injection solution.

5.2 Qualitative analysis of *lhb* in medaka embryos

Co-localization of Gfp and *lhb* were confirmed in adult medaka pituitaries. However, because the Gfp positive cells were found outside the pituitary in embryos I wanted to control that *lhb* and Gfp were expressed in the same tissue also during embryogenesis. To confirm the co-localization of *lhb* and Gfp in transgenic larvae, the most important step was the optimization of the dissection and the RNA isolation procedures. The dissection had to be quick to prevent any RNA degradation during the procedure, and carefully performed so that only Gfp positive cells were selected. The Gfp positive cells were clearly gathered in a tubular structure separate from the Gfp negative tissue. This made it possible to isolate only the Gfp positive cells using fine tweezers. To ensure no contamination of tissue from the developing pituitary in the dissected samples, RT-PCR reactions with the pituitary marker *lhx3* were performed. Several procedures were tested before the optimal procedure for collecting tissue was established. The RNA isolation procedure was performed by either placing the tissue directly in Trizol and homogenizing the sample before RNA isolation or collecting tissue in 10 µl PBS and snap freezing in liquid nitrogen before Trizol homogenization. Both of these methods were unsuccessful as they resulted in low RNA yields and variable PCR results. The procedure used in the subsequent experiments was placing the tissue directly in Cells Direct on ice after dissection. This procedure provides a quick, easy, reproducible and sensitive method for RNA extraction from small samples. Another method applied to determine the co-localization of Gfp and *lhb* was ISH. This is routinely performed in our lab, but the ISH method was not sensitive enough to detect the *lhb* in the medaka embryos. This problem was also reported from Nica et al (2006), who could neither detect *lhb* by whole mount ISH during embryonic development of zebrafish.

For imaging and qualitative analyses of the embryonic expression of Gfp-*lhb* in medaka embryos, several methods were tested to find the best protocol. For inspection of larvae with fluorescent microscope the method that was most effective and gave the best results was *in vivo* observation. The *in vivo* inspection of larvae was performed by placing the larvae in agarose wells, still in the E3 medium. The wells made it easy to stabilize the larvae and to orient them in a good position for imaging. Larvae were also anesthetized with benzocaine and dissected out of the chorion, however, this was ineffective since the larvae died shortly after dissection and were often harmed during the dissection procedure. When investigating the first expression of Gfp-*lhb* there were complications with controlling the temperature. As

medaka is a poikilotherm animal, where the internal temperature varies according to the surrounding temperature, the development of the larvae is affected by this variable. Therefore, the temperature needed to be kept constant at 27 °C. There was no incubator or heat plate available for the microscope, and therefore the room temperature was kept stable at 27 °C.

Fixation and dissection of the larvae out of the chorion was proven successful in the confocal microscope analysis and ISH analysis. Confocal imaging is time consuming and because of the movement of the larvae, *in vivo* observation could not be used during this experiment. To control that Gfp expression was not influenced by the fixation process, the larvae was observed before and after fixation. For confocal analysis, the fixed and dissected larvae were placed in a drop of agarose in a Petri dish. This was done under a dissecting microscope to control that the orientation of the larvae was optimal for analysis of the Gfp-expression and imaging. It would have been advantageous to use confocal microscopy for more advanced analysis, for example time-lapse experiments. Ideally, an experiment with time-lapse imaging of the developing larvae should have been performed, however, there was no equipment available for the upright confocal microscope to control the temperature during the time-lapse experiment, and the room temperature could not be controlled either. There was an incubator available for the inverted confocal microscope, however, a new training period was required and the optimization for inverted observation would have been too time-consuming within the scope of this master thesis. Several methods are available for improving the confocal images, for example analysis of the pictures using the Imaris program. Some of the confocal images had an insufficient resolution and restricted the analysis done with Imaris. More focus should be put to this subject in future experiments.

5.3 Quantitative analysis of *lhb* in medaka embryos

The first attempts to quantify the expression of *lhb* mRNA in medaka embryos were not successful. RNA quality is important when working with qPCR, and especially when working with low transcript levels. The RNA was analyzed for purity and degradation using the Bioanalyzer, and the RNA integrity number (RIN) values, an estimate of RNA integrity, were above eight, which indicates that most of the RNA in the sample was intact and the RNA was of good quality. This suggested that the reverse transcription step or the PCR assay needed to be optimized.

When performing a reverse transcription reaction, different primers can be used. We tested both random hexamers and Oligo(dT) primers, which binds to different parts of the RNA and can give different results. Random hexamers were initially used and when performing the qPCR experiment after a reverse transcription reaction using random hexamers, the reference gene, *bactin,* gave accurate melting curves with one specific peak and a satisfying quantification cycle (Cq) value. This confirms that the cDNA were of good quality. The *lhb* gene, however, gave very high Cq values (above 37) and the melting curves were only specific for about 50% of the samples. Random hexamers are primers that bind randomly to all RNA in the sample, including ribosomal RNA. mRNA constitutes about 10 – 20 % of the RNA in a tissue sample, and because random hexamers bind to all RNA, this can lead to a dilution effect of mRNA transcripts, especially for low abundant transcripts. The use of Oligo(dT) instead of random hexamers gave much better results. Oligo(dT) primers bind only to mRNA by annealing to the polyA tail of transcripts in the sample. The disadvantage with using Oligo(dT) primers is that if a degradation of the mRNA occurs, the primers in subsequent qPCR experiments may not detect the transcripts, as the complementary sequence for the primers may not be reverse transcribed. In addition, some transcripts do not have a polyA tail, and these transcripts will not be detected using Oligo(dT).

When working with reverse transcriptase enzymes, one should note that the sensitivity of these enzymes varies between manufacturers. The first attempts to quantify the *lhb* mRNA levels in embryonic medaka were performed using the Omniscript reverse transcriptase kit which has been shown to work well with medaka embryo RNA (K. Okubo, personal communication). Since our results in the first experiments were of poor quality, we switched to the Superscript III enzyme kit. This resulted in good quality melting curves and Cq values for both the reference gene and *lhb*. Factors that could have affected the quality of the cDNA generated with the Omniscript kit are that the enzyme could have been old or of bad quality, or the Superscript III enzyme could be more sensitive compared to the Omniscript enzyme.

To eliminate the risk of gDNA contamination, the RNA was DNase treated. The gDNA could bind to primers in subsequent qPCR assays and give inaccurate results. There are few methods of testing if the DNase treatment was successful, however, if you include a no-rt (no reverse transcriptase) in your assay, this sample will mostly include single stranded mRNA and some double stranded gDNA. Since only double stranded DNA is detected by qPCR, this will give you an indication whether the primers bind to gDNA. By performing this control,

we found that the primers used could bind gDNA and therefore DNase treatment was necessary. The DNase treatment initially used (Ambion TURBO DNase free kit, Austin, TX, USA) had an inactivation reagent that could have caused problems in our qPCR experiment. This uncertainty was solved by using Qiagen on-column DNase treatment.

Quantifying mRNA via cDNA levels as in a qPCR assay hinges on the chosen reference gene. The criteria for a good reference gene is that it should be expressed in all cells, have a constant copy number in all cells and ideally have a similar copy number as the gene of interest. *bactin* was initially used as reference gene, but it was determined to be an inappropriate reference gene since its expression varied during the developmental stages investigated. Several reference genes were tested, and *16s* was determined to be the best suited and most stably expressed.

When using Oligo(dT) instead of random hexamers, changing the reverse transcription kit from Omniscript to Superscript III and alter the reference gene for the assay performed, the qPCR experiment was successful for both the reference gene and *lhb* with a single specific melting peak and Cq values under 30.

6 Conclusion

During my study of the spatial and temporal expression of *lhb* in medaka embryos using the tg(*lhb*:GFP) medaka line, *lhb* expression was discovered in the developing gut tube. This suggests a novel function of *lhb* during embryonic development in medaka. However, the function of Lh in the intestine is still unknown and remains to be elucidated. To our knowledge, this is the first study investigating *lhb* expression during early development.

lhb is first seen in the pituitary at approximately 14 dpf, around the same time as Gnrh neurons innervate the pituitary. This suggests that Lh is expressed relatively late in development, when most of the brain morphology is established. This could mean that Lh gonadotrope cells need a final activation from the hypothalamic neurons to be activated, similar to the situation in some mammals. When *lhb* is first expressed in the pituitary, there is no expression in the gut and the yolk is completely absorbed.

The generation of a tg(*fshb*:RFP) medaka line was not completed during this master thesis. However, the tg(*fshb*:RFP) construct was successfully generated and microinjected into medaka embryos. One positive egg was discovered in the F_0 generation and this fish is now grown to sexual maturity (expected January 2012) and will be crossed with each other to identify founder fish for the transgene in the F_1 generation.

7 Future perspectives

The generation of a stable tg(*fshb*:RFP) medaka line is of great interest to the Weltzien-Haug group as a powerful tool to characterize the differential regulation of gonadotropes. The developmental studies of *lhb* expression performed in this thesis generated novel finding of great interest for developmental endocrinology. Further developmental studies of *fshb* expression in developing larvae will, therefore, also be performed to see if this hormone also has novel developmental expression and function.

When both of the transgenic lines are established, our group is planning to cross the tg(*lhb*:GFP) and the tg(*fshb*:RFP) line to generate a double tg(*lhb*:GFP,*fshb*:RFP) line of medaka. This will enable simultaneous detection and investigation of the two gonadotrope cell types. This will be a great advantage in electrophysiological experiments, Ca^{2+} imaging experiments and gene expression studies.

Subsequent studies should include elucidating the function of Lhb during development by for example knock down experiments of *lhb* and its receptor. Preliminary qPCR results from our group indicate that there is a functional ligand-receptor system for *lhb* developed already at 30-40 hpf, thus supporting the data presented in this thesis, that Lh have a function in early development.

References

Abdallah, M.A., Z.M. Lei, X. Li, N. Greenwold, S.T. Nakajima, E. Jauniaux, and V. Rao Ch. 2004. Human fetal nongonadal tissues contain human chorionic gonadotropin/luteinizing hormone receptors. *J Clin Endocrinol Metab*. 89:952-956.

Al-Kindi, A.Y., Y. Mahmoud, and M.J. Woller. 2001. Ultrastructural changes in granulosa cells and plasma steroid levels after administration of luteinizing hormone-releasing hormone in the Western painted turtle, Chrysemys picta. *Tissue Cell*. 33:361-367.

Asa, S.L., K. Kovacs, E. Horvath, N.E. Losinski, F.A. Laszlo, I. Domokos, and W.C. Halliday. 1988. Human fetal adenohypophysis. Electron microscopic and ultrastructural immunocytochemical analysis. *Neuroendocrinology*. 48:423-431.

Aubert, M.L., M. Begeot, B.P. Winiger, G. Morel, P.C. Sizonenko, and P.M. Dubois. 1985. Ontogeny of hypothalamic luteinizing hormone-releasing hormone (GnRH) and pituitary GnRH receptors in fetal and neonatal rats. *Endocrinology*. 116:1565-1576.

Ball, J.N., and B.I. Baker. 1969. The Pituitary Gland: Anatomy and Histophysiology. In: Hoar, W.S., Randall D.J. (Eds.), Fish Physiology, vol. II. The endocrine system. Academic Press, New York. Pp. 1-110.

Barbu, V., and F. Dautry. 1989. Northern blot normalization with a 28S rRNA oligonucleotide probe. *Nucleic Acids Res*. 17:7115.

Begeot, M., M.P. Dubois, and P.M. Dubois. 1982. Comparative study in vivo and in vitro of the differentiation of immunoreactive corticotropic cells in fetal rat anterior pituitary. *Neuroendocrinology*. 35:255-264.

Belvedere, P., L. Dalla Valle, S. Vianello, O. Carnevali, and L. Colombo. 2001. Hormonal steroidogenesis in liver and small intestine of the green frog, Rana esculenta L. *Life Sci*. 69:2921-2930.

Borg, B. 1994. Androgens in teleost fishes. *Comp Biochem Physiol C*. 109:219-245.

Braun, T., P.R. Schofield, and R. Sprengel. 1991. Amino-terminal leucine-rich repeats in gonadotropin receptors determine hormone selectivity. *EMBO J*. 10:1885-1890.

Bromage, N., M. Porter, and C. Randall. 2001. The environmental regulation of maturation in farmed finfish with special reference to the role of photoperiod and melatonin. *Aquaculture*. 197:63-98.

Brooks, A.N., I.S. Currie, F. Gibson, and G.B. Thomas. 1992. Neuroendocrine regulation of sheep fetuses. *J Reprod Fertil Suppl*. 45:69-84.

Burnard, D., R.E. Gozlan, and S.W. Griffiths. 2008. The role of pheromones in freshwater fishes. *J. Fish Biol*. 73:1-16.

Chang, J.P., and R.E. Peter. 1983. Effects of dopamine on gonadotropin release in female goldfish, Carassius auratus. *Neuroendocrinology*. 36:351-357.

Chang, J.P., K.L. Yu, A.O. Wong, and R.E. Peter. 1990. Differential actions of dopamine receptor subtypes on gonadotropin and growth hormone release in vitro in goldfish. *Neuroendocrinology*. 51:664-674.

Chen, J.Y., and M.J. Chiou. 2010. Molecular cloning and functional analysis of the zebrafish luteinizing hormone beta subunit (LH<beta>) promoter. *Fish Physiol Biochem*. 36:1253-1262.

Claxton, N.S., T.J. Fellers, and M.W. Davidson. 2006. Microscopy, Confocal. Encyclopedia of Medical Devices and Instrumentation. John Wiley & Sons, Inc, USA.

De Leeuw, R., C. Van 't Veer, H.J. Goos, and P.G. Van Oordt. 1988. The dopaminergic regulation of gonadotropin-releasing hormone receptor binding in the pituitary of the African catfish, Clarias gariepinus. *Gen Comp Endocrinol*. 72:408-415.

Dellovade, T., M. Schwanzel-Fukuda, J. Gordan, and D. Pfaff. 1998. Aspects of GnRH neurobiology conserved across vertebrate forms. *Gen Comp Endocrinol*. 112:276-282.

Doerr-Schott, J. 1976. Immunohistochemical detection, by light and electron microscopy, of pituitary hormones in cold-blooded vertebrates. I. Fish and amphibians. *Gen Comp Endocrinol*. 28:487-512.

Dos Santos, S., C. Bardet, S. Bertrand, H. Escriva, D. Habert, and B. Querat. 2009. Distinct expression patterns of glycoprotein hormone-alpha2 and -beta5 in a basal chordate suggest independent developmental functions. *Endocrinology*. 150:3815-3822.

Evans, D.H., and J.B. Claiborne. 2006. The Physiology of Fishes, Third edition. CRC Press, Taylor & Francis group, USA. Pp. 271-318, 343-386.

Fleige, S., V. Walf, S. Huch, C. Prgomet, J. Sehm, and M.W. Pfaffl. 2006. Comparison of relative mRNA quantification models and the impact of RNA integrity in quantitative real-time RT-PCR. *Biotechnol Lett*. 28:1601-1613.

Frisen, L. 1967. Rapid transmandibular hypophysectomy of small fish. *Experientia*. 23:1079-1080.

Garcia-Hernandez, M.P., A. Garcia-Ayala, M.T. Elbal, and B. Agulleiro. 1996. The adenohypophysis of Mediterranean yellowtail, Seriola dumerilii (Risso, 1810): an immunocytochemical study. *Tissue Cell*. 28:577-585.

Grapin-Botton, A., and D.A. Melton. 2000. Endoderm development: from patterning to organogenesis. *Trends Genet*. 16:124-130.

Herzog, W., C. Sonntag, S. von der Hardt, H.H. Roehl, Z.M. Varga, and M. Hammerschmidt. 2004. Fgf3 signaling from the ventral diencephalon is required for early specification and subsequent survival of the zebrafish adenohypophysis. *Development*. 131:3681-3692.

Herzog, W., X. Zeng, Z. Lele, C. Sonntag, J.W. Ting, C.Y. Chang, and M. Hammerschmidt. 2003. Adenohypophysis formation in the zebrafish and its dependence on sonic hedgehog. *Dev Biol*. 254:36-49.

Hildahl, J., G.K. Sandvik, R. Lifjeld, K. Hodne, Y. Nagahama, T.M. Haug, K. Okubo and F.A. Weltzien. 2011. Developmental tracing of luteinizing hormone *β*-subunit gene expression using green fluorescent protein transgenic medaka (*Oryzias latipes*) reveals a putative novel developmental function. (Submitted)

Hsu, H.J., M.R. Liang, C.T. Chen, and B.C. Chung. 2006. Pregnenolone stabilizes microtubules and promotes zebrafish embryonic cell movement. *Nature*. 439:480-483.

Hsu, S.Y., K. Nakabayashi, and A. Bhalla. 2002. Evolution of glycoprotein hormone subunit genes in bilateral metazoa: identification of two novel human glycoprotein hormone subunit family genes, GPA2 and GPB5. *Mol Endocrinol*. 16:1538-1551.

Huhtaniemi, I. 1995. Molecular aspects of the ontogeny of the pituitary-gonadal axis. *Reprod Fertil Dev* 7:1025–1035.

Iwamatsu, T. 2004. Stages of normal development in the medaka Oryzias latipes. *Mech Dev*. 121:605-618.

Japon, M.A., M. Rubinstein, and M.J. Low. 1994. In situ hybridization analysis of anterior pituitary hormone gene expression during fetal mouse development. *J Histochem Cytochem*. 42:1117-1125.

Kanda, S., K. Okubo, and Y. Oka. 2011. Differential regulation of the luteinizing hormone genes in teleosts and tetrapods due to their distinct genomic environments--insights into gonadotropin beta subunit evolution. *Gen Comp Endocrinol*. 173:253-258.

Keller, R.E. 1975. Vital dye mapping of the gastrula and neurula of Xenopus laevis. I. Prospective areas and morphogenetic movements of the superficial layer. *Dev Biol*. 42:222-241.

Kinoshita, M., K. Murata, K. Naruse and M. Tanaka. 2009. Medaka - Biology, Management, and Experimental Protocols. Wiley-Blackwell, USA. Pp. 70

Kioussi, C., C. Carriere, and M.G. Rosenfeld. 1999. A model for the development of the hypothalamic-pituitary axis: transcribing the hypophysis. *Mech Dev*. 81:23-35.

Kobayashi, D., T. Jindo, K. Naruse, and H. Takeda. 2006. Development of the endoderm and gut in medaka, Oryzias latipes. *Dev Growth Differ*. 48:283-295.

Kobayashi, M., P. Sorensen, and N. Stacey. 2002. Hormonal and pheromonal control of spawning behavior in the goldfish. *Fish Physiol Biochem*. 26:71-84.

Kumar, R.S., S. Ijiri, and J.M. Trant. 2001. Molecular biology of channel catfish gonadotropin receptors: 1. Cloning of a functional luteinizing hormone receptor and preovulatory induction of gene expression. *Biol Reprod*. 64:1010-1018.

Laiz-Carrion, R., M.M. Segura-Noguera, M.P. Martin del Rio and J.M. Mancera. 2003. Ontogeny of adenohypophyseal cells in the pituitary of the American shad (*Alosa sapidissima*). *Gen Comp Endocrinol*. 132:454-464.

Lake, J.I., H.S. Lange, S. O'Brien, S.E. Sanford, and D.L. Maney. 2008. Activity of the hypothalamic-pituitary-gonadal axis differs between behavioral phenotypes in female white-throated sparrows (*Zonotrichia albicollis*). *Gen Comp Endocrinol*. 156:426-433.

Lawson, K.A., and R.A. Pedersen. 1987. Cell fate, morphogenetic movement and population kinetics of embryonic endoderm at the time of germ layer formation in the mouse. *Development*. 101:627-652.

Levavi-Sivan, B., J. Bogerd, E.L. Mananos, A. Gomez, and J.J. Lareyre. 2010. Perspectives on fish gonadotropins and their receptors. *Gen Comp Endocrinol*. 165:412-437.

Liu, N.A., H. Huang, Z. Yang, W. Herzog, M. Hammerschmidt, S. Lin, and S. Melmed. 2003. Pituitary corticotroph ontogeny and regulation in transgenic zebrafish. *Mol Endocrinol*. 17:959-966.

Liu, N.A., M. Ren, J. Song, Y. Rios, K. Wawrowsky, A. Ben-Shlomo, S. Lin, and S. Melmed. 2008. In vivo time-lapse imaging delineates the zebrafish pituitary proopiomelanocortin lineage boundary regulated by FGF3 signal. *Dev Biol*. 319:192-200.

Lopez, M., G. Nica, P. Motte, J.A. Martial, M. Hammerschmidt, and M. Muller. 2006. Expression of the somatolactin beta gene during zebrafish embryonic development. *Gene Exp Patterns*. 6:156-161.

Millar, R.P., Z.L. Lu, A.J. Pawson, C.A. Flanagan, K. Morgan, and S.R. Maudsley. 2004. Gonadotropin-releasing hormone receptors. *Endocr Rev*. 25:235-275.

Mittelholzer, C., E. Andersson, G.L. Taranger, D. Consten, T. Hirai, B. Senthilkumaran, Y. Nagahama, and B. Norberg. 2009. Molecular characterization and quantification of the gonadotropin receptors FSH-R and LH-R from Atlantic cod (Gadus morhua). *Gen Comp Endocrinol*. 160:47-58.

Miwa, S., L. Yan, and P. Swanson. 1994. Localization of two gonadotropin receptors in the salmon gonad by in vitro ligand autoradiography. *Biol Reprod*. 50:629-642.

Naito, N., S. Hyodo, N. Okumoto, A. Urano, and Y. Nakai. 1991. Differential production and regulation of gonadotropins (GTH I and GTH II) in the pituitary gland of rainbow trout, *Oncorhynchus mykiss*, during ovarian development. *Cell Tissue Res*. 266:457-467.

Nakamura, S., D. Saito, and M. Tanaka. 2008. Generation of transgenic medaka using modified bacterial artificial chromosome. *Dev Growth Differ*. 50:415-419.

Nica, G., W. Herzog, C. Sonntag, M. Nowak, H. Schwarz, A.G. Zapata, and M. Hammerschmidt. 2006. Eya1 is required for lineage-specific differentiation, but not for cell survival in the zebrafish adenohypophysis. *Dev Biol*. 292:189-204.

Norris, D. 1997. Vertebrate endocrinology, Third edition. Academic Press, San Diego. Pp. 106-160.

Nozaki, M., N. Naito, P. Swanson, K. Miyata, Y. Nakai, Y. Oota, K. Suzuki, and H. Kawauchi. 1990. Salmonid pituitary gonadotrophs. I. Distinct cellular distributions of two gonadotropins, GTH I and GTH II. *Gen Comp Endocrinol*. 77:348-357.

Oishi, A., K. Gengyo-Ando, S. Mitani, A. Mohri-Shiomi, K.D. Kimura, T. Ishihara, and I. Katsura. 2009. FLR-2, the glycoprotein hormone alpha subunit, is involved in the neural control of intestinal functions in Caenorhabditis elegans. *Genes Cells*. 14:1141-1154.

Okubo, K., F. Sakai, E.L. Lau, G. Yoshizaki, Y. Takeuchi, K. Naruse, K. Aida, and Y. Nagahama. 2006. Forebrain gonadotropin-releasing hormone neuronal development: Insights from transgenic medaka and the relevance to X-linked Kallmann syndrome. *Endocrinology*. 147:1076-1084.

Paule, M.R., and R.J. White. 2000. Survey and summary: transcription by RNA polymerases I and III. *Nucleic Acids Res*. 28:1283-1298.

Pierce, J.G., and T.F. Parsons. 1981. Glycoprotein hormones: structure and function. *Annu Rev Biochem*. 50:465-495.

Pogoda, H.M., and M. Hammerschmidt. 2007. Molecular genetics of pituitary development in zebrafish. *Semin Cell Dev Biol*. 18:543-558.

Pogoda, H.M., and M. Hammerschmidt. 2009. How to make a teleost adenohypophysis: molecular pathways of pituitary development in zebrafish. *Mol Cell Endocrinol*. 312:2-13.

Pogoda, H.M., S. von der Hardt, W. Herzog, C. Kramer, H. Schwarz, and M. Hammerschmidt. 2006. The proneural gene ascl1a is required for endocrine differentiation and cell survival in the zebrafish adenohypophysis. *Development*. 133:1079-1089.

Pope, C., J.R. McNeilly, S. Coutts, M. Millar, R.A. Anderson, and A.S. McNeilly. 2006. Gonadotrope and thyrotrope development in the human and mouse anterior pituitary gland. *Dev Biol*. 297:172-181.

Rembold, M., K. Lahiri, N.S. Foulkes and J. Wittbrodt. 2006. Transgenesis in fish: efficient selction of transgenic fish by co-injection with a fluorescent reporter construct. *Nature Protocols*. 1:3.

Roch, G.J., E.R. Busby, and N.M. Sherwood. 2011. Evolution of GnRH: diving deeper. *Gen Comp Endocrinol*. 171:1-16.

Rocha, A., A. Gomez, S. Zanuy, J.M. Cerda-Reverter, and M. Carrillo. 2007. Molecular characterization of two sea bass gonadotropin receptors: cDNA cloning, expression analysis, and functional activity. *Mol Cell Endocrinol*. 272:63-76.

Rosenquist, G.C. 1971. The location of the pregut endoderm in the chick embryo at the primitive streak stage as determined by radioautographic mapping. *Dev Biol*. 26:323-335.

Saga, T., Y. Oota, M. Nozaki, and P. Swanson. 1993. Salmonid pituitary gonadotrophs. III. Chronological appearance of GTH I and other adenohypophysial hormones in the pituitary of the developing rainbow trout (Oncorhynchus mykiss irideus). *Gen Comp Endocrinol*. 92:233-241.

Saga, T., K. Yamaki, Y. Doi, and M. Yoshizuka. 1999. Chronological study of the appearance of adenohypophysial cells in the ayu (Plecoglossus altivelis). *Anat Embryol (Berl)*. 200:469-475.

Schreibman, M.P., J.F. Leatherland, and B.A. McKeown. 1973. Functional Morphology of the Teleost Pituitary Gland. *Amer Zool*. 13:719-742.

Schulz, R.W., and H.J.T. Goos. 1999. Puberty in male fish: concepts and recent developments with special reference to the African catfish *(Clarias gariepinus)*. *Aquaculture*. 177:5 - 12.

Segura-Noguera, M.M., R. Laız-Carriòn, M.P. Martın del Rıo, and J.M. Mancera. 2000. An Immunocytochemical Study of the Pituitary Gland of the White Seabream (Diplodus Sargus). *Histochem J*. 32:733-742.

Sellami, A., H.J. Agricola, and J.A. Veenstra. 2011. Neuroendocrine cells in *Drosophila melanogaster* producing GPA2/GPB5, a hormone with homology to LH, FSH and TSH. *Gen Comp Endocrinol*. 170:582-588.

So, W.K., H.F. Kwok, and W. Ge. 2005. Zebrafish gonadotropins and their receptors: II. Cloning and characterization of zebrafish follicle-stimulating hormone and luteinizing hormone subunits--their spatial-temporal expression patterns and receptor specificity. *Biol Reprod*. 72:1382-1396.

Szarek, E., K. Farrand, I.C. McMillen, I.R. Young, D. Houghton, and J. Schwartz. 2008. Hypothalamic input is required for development of normal numbers of thyrotrophs and gonadotrophs, but not other anterior pituitary cells in late gestation sheep. *J Physiol*. 586:1185-1194.

Takeda, H., and A. Shimada. 2010. The art of medaka genetics and genomics: what makes them so unique? *Annu Rev Genet*. 44:217-241.

Taranger, G.L., M. Carrillo, R.W. Schulz, P. Fontaine, S. Zanuy, A. Felip, F.A. Weltzien, S. Dufour, O. Karlsen, B. Norberg, E. Andersson, and T. Hansen. 2010. Control of puberty in farmed fish. *Gen Comp Endocrinol*. 165:483-515.

Tena-Sempere, M., and M.L. Barreiro. 2002. Leptin in male reproduction: the testis paradigm. *Mol Cell Endocrinol*. 188:9-13.

Thermes, V., C. Grabher, F. Ristoratore, F. Bourrat, A. Choulika, J. Wittbrodt, and J.S. Joly. 2002. I-SceI meganuclease mediates highly efficient transgenesis in fish. *Mech Dev*. 118:91-98.

Tilly, J.L., T. Aihara, K. Nishimori, X.C. Jia, H. Billig, K.I. Kowalski, E.A. Perlas, and A.J. Hsueh. 1992. Expression of recombinant human follicle-stimulating hormone receptor: species-specific ligand binding, signal transduction, and identification of multiple ovarian messenger ribonucleic acid transcripts. *Endocrinology*. 131:799-806.

Vidal, B., C. Pasqualini, N. Le Belle, M.C. Holland, M. Sbaihi, P. Vernier, Y. Zohar, and S. Dufour. 2004. Dopamine inhibits luteinizing hormone synthesis and release in the juvenile European eel: a neuroendocrine lock for the onset of puberty. *Biol Reprod*. 71:1491-1500.

Vischer, H.F., and J. Bogerd. 2003. Cloning and functional characterization of a gonadal luteinizing hormone receptor complementary DNA from the African catfish (Clarias gariepinus). *Biol Reprod*. 68:262-271.

Voss, J.W., and M.G. Rosenfeld. 1992. Anterior pituitary development: short tales from dwarf mice. *Cell*. 70:527-530.

Wallace, K.N., and M. Pack. 2003. Unique and conserved aspects of gut development in zebrafish. *Dev Biol*. 255:12-29.

Wallace, K.N., Akthter S., Smith E.M., Lorent K., Michael P. 2005. Intestinal growth and differentiation in zebrafish. *Mechanisms of Development*. 122:157-173

Wells, J.M., and D.A. Melton. 1999. Vertebrate endoderm development. *Annu Rev Cell Dev Biol*. 15:393-410.

Weltzien, F.A., C. Pasqualini, P. Vernier, and S. Dufour. 2005. A quantitative real-time RT-PCR assay for European eel tyrosine hydroxylase. *Gen Comp Endocrinol*. 142:134-142.

Weltzien, F.A., E. Andersson, O. Andersen, K. Shalchian-Tabrizi, and B. Norberg. 2004. The brain-pituitary-gonad axis in male teleosts, with special emphasis on flatfish (pleuronectiformes). *Comp Biochem Physiol A.* 137:447-477.

Weltzien, F.A., B. Norberg, J.V. Helvik, O. Andersen, P. Swanson, and E. Andersson. 2003. Identification and localization of eight distinct hormone-producing cell types in the pituitary of male Atlantic halibut (Hippoglossus hippoglossus L.). *Comp Biochem Physiol A.* 134:315-327.

Wong, A.C., and A.L. Van Eenennaam. 2004. Gonadotropin hormone and receptor sequences from model teleost species. *Zebrafish*. 1:203-221.

Yan, H.Y., and P. Thomas. 1991. Histochemical and immunocytochemical identification of the pituitary cell types in three sciaenid fishes: Atlantic croaker (Micropogonias undulatus), spotted seatrout (Cynoscion nebulosus), and red drum (Sciaenops ocellatus). *Gen Comp Endocrinol*. 84:389-400.

Yan, L., P. Swanson, and W.W. Dickhoff. 1992. A two-receptor model for salmon gonadotropins (GTH I and GTH II). *Biol Reprod*. 47:418-427.

Yu, K.L., P.M. Rosenblum, and R.E. Peter. 1991. In vitro release of gonadotropin-releasing hormone from the brain preoptic-anterior hypothalamic region and pituitary of female goldfish. *Gen Comp Endocrinol*. 81:256-267.

Zhou, L.Y., Wang, D.S., Shibata, Y., Paul-Prasanth, B., Suzuki, A., Nagahama, Y. 2007. Characterization, expression and transcriptional regulation of *P450c17-I* and *–II* in the medaka, *Oryzias latipes. Biochem Biophys Comm.* 362:619-625

Zhu, X., A.S. Gleiberman, and M.G. Rosenfeld. 2007. Molecular physiology of pituitary development: signaling and transcriptional networks. *Physiol Rev*. 87:933-963.

Zhu, Y., J.W. Stiller, M.P. Shaner, A. Baldini, J.L. Scemama, and A.A. Capehart. 2004. Cloning of somatolactin alpha and beta cDNAs in zebrafish and phylogenetic analysis of two distinct somatolactin subtypes in fish. *J Endocrinol*. 182:509-518.